MARCELLUS SHALE PRODUCED WATER TREATMENT BY DIRECT CONTACT MEMBRANE DISTILLATION WITH ACRYLIC COPOLYMER MEMBRANES

by

Emily Wolff

B.S. in Civil Engineering, University of Pittsburgh, 2011

Submitted to the Graduate Faculty of

Swanson School of Engineering in partial fulfillment

of the requirements for the degree of

Master of Science

University of Pittsburgh

2016

UNIVERSITY OF PITTSBURGH

SWANSON SCHOOL OF ENGINEERING

This thesis was presented

by

Emily Wolff

It was defended on

November 10, 2016

and approved by

Radisav D. Vidic, Ph.D., Professor, Department of Civil and Environmental Engineering

Leonard W. Casson, Ph.D., Associate Professor, Department of Civil and Environmental Engineering

Vikas Khanna, Ph.D., Assistant Professor, Department of Civil and Environmental Engineering

Thesis Advisor: Radisav D. Vidic, Ph.D., Professor, Department of Civil and Environmental Engineering

Copyright © by Emily Wolff

2016

MARCELLUS SHALE PRODUCED WATER TREATMENT BY DIRECT CONTACT MEMBRANE DISTILLATION WITH ACRYLIC COPOLYMER MEMBRANES

Emily Wolff, M.S.

University of Pittsburgh, 2016

Membrane distillation (MD) is a promising treatment solution that can provide the oil and gas industry an efficient and cost effective desalination treatment method for flowback and produced waters. This will allow the industry to look beyond deep well injection and reuse as the chief water disposal management practices. A potential setback of MD treatment for oil and gas wastewater applications is that volatile organic compounds can degrade the hydrophobicity of membranes most commonly used in MD, which would allow salt breakthrough into the permeate. To overcome this setback, an acrylic copolymer hydrophobic membrane with oleophobic properties was selected for MD treatment of flowback and produced waters using a direct contact membrane distillation module.

Experimental runs with this module were conducted with pure sodium chloride solutions as well as with synthetic and actual flowback/produced waters at different TDS concentrations. The acrylic copolymer membrane had a permeate flux of 30.1 kg/m^2hr for 3.5% NaCl solution which is comparable to other hydrophobic membranes that have been widely accepted by the MD industry. There was little observable difference between the permeate flux measured using pure sodium chloride, synthetic flowback, and actual flowback when comparing equivalent percent salt concentrations. The permeate flux decreased with TDS increase. The permeate flux increased as the temperature difference between the hot feed and cold permeate side decreased for all waters tested. Both 0.2 and 0.45μm nominal pore size acrylic copolymer membranes

were studied with the 0.45 µm performing marginally better for flux production while the 0.2 µm membrane seemed to be more effectively rinsed. For all experiments conducted there were no signs of pore wetting and ionic breakthrough and the initial longevity test results are positive indicating that MD treatment for oil and gas wastewater applications may be viable.

Keywords: Direct Contact Membrane Distillation (DCMD), Marcellus Shale, Flowback water, Produced water, Acrylic Copolymer Membrane

TABLE OF CONTENTS

LIST OF TABLES

LIST OF FIGURES

ACKNOWLEDGMENTS

I wish to express my sincere gratitude to my supervisor Dr. Radisav Vidic, for the opportunity to continue my studies at the University of Pittsburgh and for his direction in my master program. His guidance, persistence, and acumen were crucial contributions towards the successful completion of my graduate studies. I would also like to acknowledge Dr. Leonard Casson and Dr. Vikas Khanna for their support and input as members of my thesis defense committee.

I owe a debt of gratitude to Dr. Elise Barbot who assisted with my initial module design and offered me help and sagely advice during my time as both an undergraduate and graduate student researcher. I am also grateful to Dr. Shiyun Zhu for her initial work with membrane distillation at the University of Pittsburgh and to Dr. Jason Monnell for his support and guidance with my research, scholarly, and professional pursuits.

I am very grateful to my graduate student colleagues and friends, Brad Harken, Huiqi Deng, Jason Lee (the angel of my contact angles), Wenshi Lui, Tieyuan Zhang, Xuan Zheng, and Can He for their help and reinforcements with my graduate studies and thesis work. I am also thankful for my coworkers at both Aquatech and GAI Consultants' encouragement to complete my thesis work. Finally, I would also like to thank to my friends, roommates, family and my boyfriend Danny Lynch for their love, support and gentle reminders to keep my eye on the prize over the years.

1.0 INTRODUCTION

The development of horizontal drilling coupled with hydraulic fracturing has stimulated a great deal of investment and activity for recovery of natural gas from unconventional sources (i.e., on-shore shale plays). While various shale plays in the U.S. and elsewhere have long been known to contain natural gas, these technological accomplishments have now made it economically attractive to develop these natural gas resources. These advancements brought a surge in gas exploration, including the development of the Marcellus Shale formation in parts of Pennsylvania, West Virginia and Ohio.

Both the quantity of water that is required for hydraulic fracturing, and the quality of flowback and produced water associated with the development of shale gas resources has raised many environmental concerns. On average, 3.8 million gallons of water is necessary to hydraulically fracture a single horizontal well in the Marcellus Shale formation (Hayes, 2009). Approximately 10-30% of this water returns to the surface as flowback within 2 weeks of fracturing the well. According to the PADEP Office of Oil and Gas from January 1, 2005 through October 14, 2016, over 21,000 unconventional oil and gas drilling permits have been issued in Pennsylvania. During that same period, 12,235 unconventional wells were drilled in Pennsylvania (Pennsylvania Department of Environmental Protection, 2016). In late 2014, the prices of crude oil and natural gas dropped significantly, and the rate of oil and gas drilling in Pennsylvania dropped with it, as the costs associated with well development began to exceed returns. That said, many producers have continued to drill wells despite the low prices, often times to maintain leases and /or as part of their water management plan.

One of the most remarkable characteristics of the flowback water is that the total dissolved solids (TDS) content can reach 100,000 mg/L, three times the average TDS concentration in seawater, while the produced water in Marcellus Shale can reach 300,000mg/L TDS. Sodium and chloride are the primary ions present, followed by calcium, barium, strontium and magnesium and varies by what part of the Marcellus Shale play the water is generated. The water also contains heavy metals at low concentrations. Many of the flowback water TDS constituents can have significant adverse impact on both human health and environment (even low toxicity constituents can have impact at sufficiently high concentrations), especially if the flowback water is not managed properly.

The high concentrations of suspended and dissolved constituents preclude direct discharge of flowback water into receiving streams. Effluent limitation guidelines by the USEPA specify zero discharge of untreated wastewater associated with onshore oil and gas extraction into navigable waters (Title 40, Part 435 of the Code of Federal Regulations). Some publicly owned treatment works (POTWs) benefited from existing NPDES permits which allowed them to treat “pretreated” flowback water at up to 1% of their average flowrate but due to intense public scrutiny POTWs can no longer accept flowback water. There are a number of permitted industrial wastewater treatment facilities which can treat and dispose waters from the oil and gas industry, but they can only accept and discharge waters derived from unconventional wells (Marcellus Shale included) if they treat to less than 500 mg/L TDS. Currently, most producers opt to reuse the wastewater for hydraulic fracturing of further wells or dispose of it in government-regulated deep well injection locations.

The chief method for ultimate disposal of wastewaters associated with Marcellus Shale natural gas play is through deep well injection. In Pennsylvania there are currently only eight

permitted Class II Underground Injection Control wells, which are able to accept wastewater from the oil and natural gas industry. There are 217 active Class II wells in Ohio, any of which can accept wastewater from Pennsylvania hydraulic fracturing events (Ohio Department of Natural Resources, 2016). However, deep well injection practices may not remain an accepted form of disposal for much longer due to suspected links between increased injection well activity and recent earthquakes in Ohio. There were eleven recorded earthquakes in Ohio in late 2011, including a magnitude 4.0 earthquake in Youngstown, Ohio. According to experts at Columbia University, evidences suggest a likely correlation between that earthquake and the local deep well injection activity. The well in suspect was shut down by regulators shortly after the larger earthquake (https://www.ldeo.columbia.edu/news-events/seismologists-link-ohio-earthquakes-waste-disposal-wells, 2012). Even if deep well injection is found to be unrelated to the recent increased seismic activity on the east coast, many are beginning to question the integrity and ability of these wells to remain secure in the event of a major earthquake.

To reduce the amount of water that needs to be disposed of as well as the amount of freshwater used in hydraulic fracturing, shale gas development companies are striving to reuse most of the flowback water in hydraulic fracturing events. Flowback and produced water reuse is feasible only as long as there is sufficient number of new wells where this water can be utilized for hydraulic fracturing, which is not necessarily the case for mature fields. It has become increasingly evident that the future of the unconventional onshore gas industry is critically dependent on technical solutions that would enable efficient and cost effective management of flowback and produced waters beyond deep well injection and reuse. This study is designed to evaluate membrane distillation (MD) technology to meet this objective and to produce a low TDS permeate which could be permitted for discharge.

The extremely high TDS concentrations render reverse osmosis (RO), the most prevalent desalination technology employed for seawater desalination, ineffective for use in treating these complex shale gas wastewaters. High salinity of the feed water decreases the driving force for mass transport in RO considerably but has minimal impact on MD because of the limited impact on vapor pressure of water, which is the driving force in MD (Cath et al., 2004). Complete rejection of ions and dissolved non-volatile organics is achieved with MD as long as the membrane pores are not wetted (Nghiem and Cath., 2011). The other principal advantage of MD over other treatment technologies is a much lower expected energy demand because MD can effectively operate at near atmospheric pressure and in the temperature range of 50-100^{o}C, which is significantly lower than typical temperatures used in conventional thermal treatment processes (e.g., distillation, mechanical vapor recompression). As a result, associated costs with MD are predicted to be drastically lower than their thermal and membrane processes counter-parts, (Al-Obaidani et al., 2008; Macedonio, 2010).

1.1 OBJECTIVES

The present research focuses on clean water yields of membrane distillation from both synthetic and actual flowback/produced waters under conditions that are relevant in practical applications. The overall objectives of this work include:

1. Investigate the feasibility of membrane distillation as a final treatment method for flowback/produced waters from the Marcellus Shale natural gas play.

2. Investigate whether acrylic copolymer hydrophobic membranes are suitable for membrane distillation of flowback/produced water, in terms of chemical compatibility and performance characteristics.

1.2 APPROACH

In this study, a flat sheet, direct contact membrane distillation (DCMD) module with a membrane contact surface area of 0.004 m^2 was constructed to test the feasibility of MD technology for treating flowback and produced water from unconventional gas extraction in Marcellus shale. Experimental runs with this module were conducted with synthetic and actual flowback/produced waters at different concentrations to explore how these variances affected permeate flux. To keep the feed water chemistry as the primary independent variable, experiments were completed within the same feed temperature range and with the same acrylic copolymer (AC) membrane. The effect of membrane pore size on MD flux was also investigated, with most feed water chemistry experiments being conducted with both 0.2µm and 0.45µm AC membranes. For AC membranes to be a viable membrane choice for this application, they must maintain performance over time, within the harsh chemistries of flowback water. Therefore the longevity and the fouling and scaling potential were chosen as measures of AC membrane performance. Rinsing effectiveness was briefly examined to see if the clean water fluxes could be returned to pristine levels after experiments with flowback/produced water. Also following experimental runs, the used membranes were then examined with SEM/EDX to characterize the crystals that formed on the membrane surface.

2.0 THEORETICAL REVIEW

Although this treatment technology was first patented in the 1960s it is still being actively investigated by the academic community and has seen little commercial application. Therefore, it is worthwhile to present here the current state of membrane distillation technology and the basic concepts and calculations used in this study.

2.1 WHAT IS MEMBRANE DISTILLATION

Membrane distillation is a separation process that combines thermal and membrane separation methods. The driving force behind the desalting of saline waters in MD is the difference in vapor pressure caused by a temperature differential between the hot feed stream and the cold distillate stream, which are separated by a microporous, hydrophobic membrane. This vapor pressure difference causes water evaporation on the hot feed side and transfer of pure water vapor through the hydrophobic membrane leaving the solute ions in solution on the feed side. The pure permeate water vapor is then recovered once it condenses in the cold distillate stream.

There are four existing MD configurations: direct contact membrane distillation (DCMD) where permeate is condensed directly on the membrane surface, vacuum membrane distillation (VMD) requiring a vacuum pump on the permeate side, sweep-gas membrane distillation (SGMD) which is equipped with a condenser on the permeate side, and air-gap membrane

distillation (AGMD) where permeate is condensed on a cooling surface. DCMD, which was selected for this study, has the simplest operation configuration and is the most widely studied. Fig. 1, illustrates that the hot feed and cold permeate streams are in direct contact with the membrane surface. Generally DCMD is operated using a cross flow pattern and can be applied with either flat sheet or hollow fiber membranes (El-Bourawi et al., 2006). Utilizing hollow fiber modules combines large membrane surface area with a small footprint and is thus the preferred configuration in pilot plant scaling studies (Sirkar and Song, 2009).

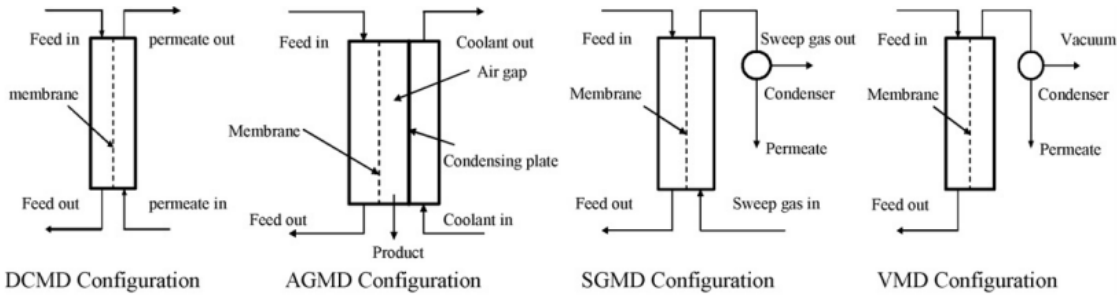

Figure 1. Different Types of MD Configurations (El-Bourawi et al., 2006)

Membrane distillation is appealing for desalination applications due to high rejection factors (for waters containing no volatile solutes) and ability to treat waters with very high salinity. Near 100 percent rejection of ions and dissolved non-volatile organics is achieved with MD as long as the membrane pores are not wetted; wetted membrane pores lead to pore flooding – the liquid intrusion of water through the membrane and subsequent ion breakthrough (Nghiem and Cath, 2011). MD is able to effectively treat higher concentration feed streams than RO because the increased concentrations only slightly decreases the vapor pressure of water, (the driving force of mass transfer in MD) while the increased concentration considerably decreases the driving force for mass transport in RO (Cath et al., 2004).

2.2 MEMBRANE DISTILLATION THEORY AND OPERATING EFFECTS

This section reviews the heat and mass transfer principles as they are applied to MD and how different operating parameters influence MD performance.

2.2.1 Heat and Mass Transfer in MD

As previously stated, the driving force behind MD is the difference in vapor pressure that is caused by a temperature gradient between the hot feed and the cold distillate streams. One can enhance the permeate flux performance in MD by increasing the driving force (increasing the difference in vapor pressure) and/or by lowering the mass transfer resistance. The mass transfer resistance has been found to have greater impact on permeation flux than variances in the driving force (Wang et al., 2011).

2.2.1.1 Heat Transfer in MD

The temperature difference across the membrane directly induces the required vapor pressure difference to drive transmembrane flux in a DCMD (Khayet, 2011). This relationship is governed by the Antoine equation:

$$P = 10^{\left(A - \frac{B}{T+C}\right)} \quad (1)$$

where, P is the vapor pressure in bar, T is the temperature in K, and A, B, C are the Antoine equation parameters. For pure water ranging in temperature from 304-333 K, A=5.20389, B=1733.926, and C=-39.485, (P.J. Linstrom and W.G. Mallard, 2016). As temperature increases vapor pressure exponentially increases.

A basic understanding of the heat transfer involved in MD is important to enhance permeate production efficiently. Heat transfer in MD occurs in three steps: i) transport through the feed boundary layer by convection, ii) transport through the membrane by conduction and by the latent heat of vaporization, iii) transport through the permeate boundary layer by convection (Alkhudhiri et al., 2012). The heat flux in MD occurs by two major mechanisms: i) the latent heat transfer that accompanies the vapor flux and ii) the conductive heat transfer through the membrane. The second mechanism is not considered useful heat transfer (it is a heat loss in the system) and it should be minimized to increase process efficiency. It has been found that usually 50 to 80% of the total heat flux in MD is due to the latent heat (Schofield et al., 1987).

Thermal efficiency in MD is defined as the ratio of latent heat of vaporization to the total heat, which includes both latent and conductive heat. This efficiency decreases as the concentration of the feed solution rises. Thermal efficiency can be increased with higher feed temperatures, higher feed flow rates, and thicker membranes (Al-Obaidani et al., 2008). However, the mass transfer resistance typically has the highest impact on flux performance and the membrane thickness does contribute to this resistance. Al-Obaidani et al. has an excellent discussion on balancing the various membrane characteristics and operating parameters to optimize flux production. Some of these points will be further discussed in Section 2.2.3.

2.2.1.2 Mass Transfer in MD

The transport of volatiles (water vapor) through the membrane pores in MD happens due to convection and diffusion. There are three different controlling mechanisms that govern the mass transfer resistance through the membranes in MD. They are Knudsen diffusion, molecular diffusion, and Poiseuille flow (viscous flow). Knudsen diffusion occurs in MD applications when the pore sizes are small and it is a measure of mass transport resulting from the molecule-pore

wall collisions. Molecular diffusion is a measure of mass transport resulting from molecule-molecule collisions and is under the influence of the molecular concentration gradient. In most MD applications both Knudsen and molecular diffusion occur concurrently. When the pore size diameter is particularly small (less than 0.14µm at 50°C and atmospheric pressure) Knudsen diffusion dominates. Conversely when the pore size diameter is particularly large (greater than 14µm at 50°C and atmospheric pressure) molecular diffusion dominates. Mass transport deriving from Poiseuille flow is when the molecules are driven by a pressure gradient, (Alkhudhiri et al., 2012; Khayet, 2011).

Several theoretical models have been developed for the mass transport in MD but the dusty gas model is most generally used (Khayet, 2011). The dusty gas model combines the three aforementioned mechanisms and was first applied by Lawson and Lloyd for DCMD (1997).

$$\frac{J_i^D}{D_{ie}^k} + \sum_{j=1\neq i}^{n} \frac{p_i J_i^D - p_i J_j^D}{D_{ije}^O} = -\frac{1}{RT}\nabla p_i \text{ and } J_i^V = -\frac{B_o p_i}{RT\mu}\nabla P \quad (2)$$

where, J^D referrers to the diffusive type of flux, J^V is the viscous type of flux, and the total flux is $J_i = J^D + J^V$, P is the total pressure, p_i is the partial pressure of component i, μ is the fluid viscosity, and B_o is a constant based on membrane characteristics. D_{ie}^k is the effective Knudsen diffusion coefficient, and D_{ije}^O is the effective ordinary diffusion coefficient and both can be defined as:

$$D_{ie}^k = K_0\left(\frac{8RT}{\pi M_i}\right)^{1/2} \text{ and } D_{ije}^O = K_1 P D_{ij} \quad (3)$$

where, $\left(\frac{8RT}{\pi M_i}\right)^{1/2}$ is the mean molecular speed, D_{ij} is the ordinary diffusion coefficient, and K_o and K_1 are constants that depend on the membrane characteristics. B_o, K_o, and K_1 can all be determined experimentally or from the membrane pore radius, tortuosity, and porosity assuming that membrane consists of uniform cylindrical pores.

The dusty gas model was first used by Maxwell in the 1800s to describe the diffusion through a porous media for isothermal systems. Lawson and Lloyd showed that even though MD is a non-isothermal process that the dusty gas model is still applicable when the average temperature across the membrane, T_{avg}, replaces the T found in Maxwell's equations (Khayet, 2011; Lawson and Lloyd, 1997).

The mass flux, J, in MD is proportional to the vapor pressure difference across the membrane:

$$J = C_m[P_{m,f} - P_{m,p}] \tag{4}$$

where, C_m is the membrane distillation coefficient and $P_{m,f}$ and $P_{m,p}$ are the vapor pressures at the membrane feed and permeate surfaces. The membrane coefficient accounts for the membrane characteristics that cause the mass transfer resistance, (such as mean pore size, membrane thickness, pore tortuosity to name a few). Some of these effects are individually captured in the dusty gas model and other more complex models for predicting flux in MD applications (Alkhudhhiri et al., 2012).

The flux in MD is experimentally determined by measuring the amount of permeate collected during a predetermined period of time. The fluxes reported in the results portion of this thesis utilize this fundamental definition of mass flux.

2.2.1.3 Temperature and Concentration Polarization

The theories discussed above are the basis for understanding the MD process. However, to take this understanding to a deeper level it is pertinent to know that there are both temperature and concentration polarization phenomena which occur during MD operation. These polarization phenomena arise because the temperature and concentration profiles change inside the module as one moves from the bulk liquid stream to the membrane surface. This is illustrated in Figure 2.

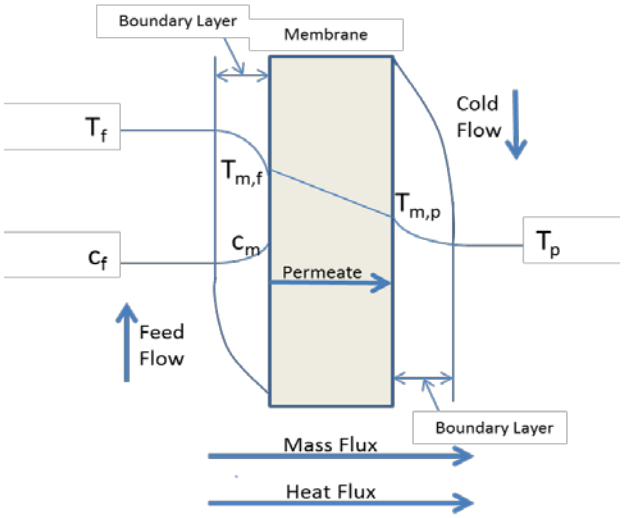

Figure 2. Temperature and Concentration Polarization in DCMD

Temperature polarization occurs on both sides of the membrane in DCMD because the water phase transformations take place on both membrane surfaces (vaporization and condensation). The temperature polarization, ψ, is defined as:

$$\psi = \frac{T_{mf} - T_{mp}}{T_f - T_p} \tag{5}$$

where, T_f and T_p are the temperatures of the bulk feed and permeate solutions; and T_{mf} and T_{mp} are the interfacial temperatures on the membrane surface on the feed and permeate sides

respectively. When this value approaches 0, it means that there is a high degree of temperature polarization. Conversely, a value that approaches 1 indicates that the difference between the temperature of the liquid-vapor interface at the membrane surface and the bulk liquid temperature is small. This value usually falls between 0.4-0.7 in DCMD applications (Alkhudhiri et al., 2012). The bulk temperatures are the thermal driving force and they contribute to interfacial temperatures which are the mass transfer driving force; thus, it is important to account for temperature polarization when calculating the vapor pressures and predicting flux using Equation 4, (Schoefield et al., 1987).

The concentration polarization only occurs on the feed side of the membrane, because there shouldn't be any measureable concentrations of dissolved species in the permeate if MD is working properly. The concentration polarization, Φ, is defined as:

$$\Phi = \frac{c_m}{c_f} \tag{6}$$

where, c_m is the is the concentration on the membrane surface and c_f is the concentration in the bulk solution (Alkhudhiri et al., 2012). When this value approaches 1 it indicates that there is little difference between the concentration on the membrane surface and the bulk solution. When this value is greater than 1, it means that there is a greater concentration polarization effect. This is significant because even if the bulk solution is below the ionic super saturation concentration it could be at super saturation on the membrane surface, which could lead to crystallization directly on the membrane surface. At high salinity, concentration polarization can become a critical limiting step for mass transfer in MD applications; however increasing the feed flow rate and

feed temperature can reduce the effect of concentration polarization and enhance the flux, (Yun et al., 2006). If the concentration on the membrane surface remains at supersaturation, crystallization may clog membrane pores and completely suppress the membrane permeability (Tun et al., 2005).

2.2.2 Operating Parameters

MD performance can vary greatly if care is not taken to normalize the operating parameters. In this section several MD operating parameters are discussed with an emphasis on how they affect MD flux performance. The three parameters that most directly impact the permeate flux in MD are the membrane properties, feed temperature, and feed concentration.

2.2.2.1 Membrane Properties

Foremost, the membranes utilized in MD applications must be hydrophobic to prevent liquid from passing through the pores along with the water vapor to keep the ions in the feed solution separate from the cold distillate stream. Polytetrafluoroethylene (PTFE), polypropylene (PP), and polyvinylidene fluoride (PVDF) are the most commonly studied hydrophobic membranes utilized in MD applications.

Liquid entry pressure (LEP), or wetting pressure, is a critical characteristic of MD membranes. LEP is defined as the minimum pressure that needs to be applied in order for distilled water to overpower the hydrophobic forces of the membrane and thus enter, or “wet,” the membrane pores and produce a continuous flux through the membrane. High LEPs are desired in MD processes to ensure consistent permeate quality (Smolders and Franken, 1989).

The LEP and permeability of a membrane are both highly dependent on the membrane pore size. Generally flux increases with pore sizes because the mass transfer is no longer dictated by Knudsen diffusion so there is an increase in permeability (Cath, 2004). Smaller membrane pore sizes result in higher LEPs which helps ensure better distillate quality, but they also result in lower production rates (Khayet, 2011). Therefore, when selecting a membrane pore size for MD applications it must be considered whether the application needs to be optimized for production rates or distillate quality. In DCMD applications, the selected maximum pore size is typically between 0.1-0.6 μm (Alkhudhiri et al., 2012).

Porosity, which is the void volume fraction of the membrane, is directly proportional to membrane permeability in MD as it is in most membrane applications. Higher porosity means that there is more pore space available for water vapor to pass through the membrane, thus leading to higher flux (Adnan et al.,2012; Khayet, 2011).

Membrane thickness also has significant impact on MD performance. The thicker membranes are more mechanically robust, thereby allowing operations at higher flow rates and pressures (Smolders and Franken, 1989). It was alluded to in the heat and mass transfer section of this review that membrane thickness is a parameter which must be delicately balanced beyond specific strength requirements. The mass transfer resistance increases with thicker membranes because the water vapor has a longer distance to travel before it can be condensed, which reduces the permeate flux. However, thicker membranes result in lower conductive heat transfer through the membrane which increases the thermal efficiency of the MD process. One study found that the optimal membrane thickness for DCMD applications is between 30-60μm (Lagana et al., 2000).

Membranes used in MD are generally more resistant to oxidation and are more chemically inert than RO membranes but the lifetime of membranes used in full scale MD applications is predicted to be similar to that of membranes used in RO processes. Scaling and fouling still occur with MD as with other membrane processes (RPSEA Project 07122-12, 2009). However, because MD is not pressure driven, the scale layers are not compacted on the membrane surface and they are much easier to remove. Periodic rinsing of the membrane surface with clean water has been sufficient in restoring membrane performance for DCMD seawater desalination purposes at the pilot scale level (Song et al., 2008). Softening pretreatment has also been found successful in diminishing scaling effects of $CaSO_4$ and SiO_2 formation (Martinetti et al., 2009).

2.2.2.2 Feed Temperature

It has been previously stated in this review several times that the temperature influences the vapor pressure and that the difference in vapor pressure is what drives the mass transfer in MD. Thus the operating temperatures of the feed and permeate streams are both important operating parameters.

Operating feed temperature is arguably the most critical parameter in affecting permeate flux in the MD process because vapor pressure increases exponentially with temperature in accordance with the Antoine equation as discussed in Section 2.2.1.1. Thus, increasing the feed water temperature results in an exponential increase in the permeate flux. The feed temperature influences the flux more than the permeate temperature because the vapor pressure increases more at higher temperatures (Alkhudhiri et al., 2012). After conducting thorough exergy, cost, and sensitivity analysis, Al-Olbaidani et al. concluded that an operating feed temperature of 55˚C was optimal for their DCMD model (2008).

2.2.2.3 Feed Concentration

Increasing the feed stream's ionic concentration decreases the flux production because it decreases the vapor pressure (Alkhudhiri et al., 2012). However, the decreases in flux are negligible and the flux is nearly constant up to 73 -76 g/L of NaCl (Martinetti et al., 2009; Cath et al., 2004). Theoretically, this makes MD a much more attractive treatment process over RO for highly saline waters. If the feed concentration is raised from distilled water to 70 g/L NaCl, the driving force in RO systems would decrease more than 85 percent while the driving force in MD would only drop approximately 2 percent (Cath et al., 2004).

Raoult's law states that the partial vapor pressure of each component of an ideal mixture of liquids is equal to the vapor pressure of the pure component multiplied by its mole fraction in the mixture. Thus as the salinity increases, the mole fraction of pure water decreases, and the vapor pressure decreases. As a general rule, Raoult's law can be applied in MD applications, however as the salinity increases, the assumption of an "ideal" solution can no longer be accurately applied due to interactions from the salt ions interfering with evaporation (Alklaibi and Lior, 2005). Vapor pressure can be determined from Raoult's law for dilute solutions, but for higher solutions it, actual vapor pressure tend to show a negative deviation from Raoult's law and it is better to have experimental measurements, (Sharqawy, 2010).

2.2.2.4 Feed Flow Rate

Feed flow rate also has an affects MD flux performance. Increasing the flow rate decreases the concentration and temperature polarization affects by keeping the fluids well mixed. By decreasing the temperature polarization affect, the heat mass transfer coefficient is maximized. This is because the flow rate enhances the mixing to keep the interfacial temperature closer to that of the bulk feed temperature, thus increasing the transmembrane difference, which directly

increases the flux production. This correlation has been widely documented (Alkhudhiri et al., 2012; Cath et al., 2004; Holman, 1986; Kays and Crawford; 1993; Schofield et al., 1990; Yun et al., 2006). When the concentration polarization impact is minimized by high feed velocities, especially in high feed salt concentrations, the likelihood of crystallization on membrane surface is also minimized.

2.3 STATE OF MEMBRANE DISTILLATION TECHNOLOGY IN INDUSTRY

Interest in MD technology is growing throughout the realms of academia and industry. Even though, it took some time for membrane technology to catch up with the concepts behind MD, the field is now rapidly developing. From rudimentary desalination enhancement, to refined theoretical modeling, to controlled crystal growth environments, to membrane coatings, the study and applications of MD seem to be expanding in all directions.

While there are still a number of potential theoretical research areas to be undertaken, there is a need for more research and developmental studies to bring MD technology to the industrial and commercial markets. There are limited studies on high salt applications, long term operations, industrial water treatment applications and full scale pilot studies published in the MD field.

A DCMD model developed by Song et al. (2008), successfully predicted the permeate production for scaling up MD modules with membrane surface areas of 119 cm^2 to 0.28 m^2 up to a series of modules with 6.6 m^2 toal membrane surface area. This is promising because it shows that MD models may be able to accurately predict flux production allowing one to estimate

system recovery and costs for full scale operations. Several other research groups have estimated costs for MD plants by extrapolating from bench scale and pilot studies. Table 1 details a summary of these cost estimates.

Table 1. Summary of estimated MD costs in literature

Water Cost (USD/m^3)	**System Description***	**Year**	**Reference**
1.17	MD with heat recovery	2007	Al-Olbaidani, 2008
0.64	MD using low-grade heat source	2007	Al-Olbaidani, 2008
0.56	NF + RO with ERD and MD with available heat energy	2007	Macedonio, 2007
0.8	NF + RO without ERD and MD with available heat energy	2007	Macedonio, 2007
0.73	NF + RO with ERD and MD without available heat energy	2007	Macedonio, 2007
0.97	NF + RO without ERD and MD without available heat energy	2007	Macedonio, 2007
0.27	MD using industrial waste heat	2006	Hanemaaijer, 2006
1.25	RO + MD	2004	Alklaibi and Lior, 2004
1.32	MD only	2004	Alklaibi and Lior, 2004
0.78	MD with ERD and without available heat energy	2003	Sirkar and Li, 2003

*NF is nanofiltration and ERD is energy recovery device

The average estimated cost of producing water from MD is \$0.85/m^3. The majority of these cost evaluations conclude that MD is economically competitive with existing desalination technologies, namely RO. For example, one particular study completed capital and O&M cost estimates for a 1MGD DCMD plant and estimated that the production cost of water for DCMD would be \$2.97 per kgal, which is significantly less than the reported costs for an RO plant of the same capacity \$4.48 USD per kgal, (Sirkar and Li, 2003). Costs for MD should be lower than RO especially if a low-grade heat energy source (waste or solar) is available to heat the feed stream in the plant, (Al-Obaidani et al., 2008).

There are only a few companies advertising and promoting MD technology commercially at this time. SolarSpring GmbH focus on solar thermal desalination systems and are marketing a "MMD" system based on MD, (http://www.solarspring.de/index.php?id=19, 2016). Blue Gold Technologies, is marketing an MD system commercially in the United States. Their system is called Memstill™ which is an AGMD module that was developed and patented by Keppel Seghers, (http://bluegoldtech.com/technology/, 2016), (http://www.keppelseghers.com/en/content.aspx?sid=3023, 2016). Limited data is publicly available about the unit and their pilot results but they advertise that desalination costs for the process could be as low as 0.5 USD/m^3, (Hanemaaijer et al., 2006). SCARB HVR (http://www.hvr.se/Products.html, 2016) is a Swedish frim and has developed an AGMD system and have made stand-alone, table top prototypes that they intend to bring to the market for drinking water systems. Another MD producer, memsys[1] (http://www.memsys.eu/, 2016) partnered with Aquaver (http://www.aquaver.com/, 2016) and with GE (http://www.memsys.eu/partners-details/ge.html, 2016). GE has conducted a pilot scale test utilizing a mechanical vapor compression driven MD (MVC-MD) system in Texas treating produced water from the oil and gas industry, (http://www.chemicalprocessing.com/vendor-news/2013/ge-and-memsys-field-project-shows-promise-for-treatment-of-fracking-wastewater/, 2016), (Silva et al., 2014).

A Technical Assessment of Produced Water Treatment Technologies (RPSEA Project 07122-12, 2009) assessed the applicability of MD for produced water treatment as "moderate to good" and the Society of Petroleum Engineers concluded that MD "may have potential in the longer term" in their assessment of advanced water treatment technologies to treat produced

[1] memsys is the official company name (with lower case "m")

water from the petroleum industry (Dores et al., 2012). The hesitations in these assessments stem from the lack of literature supporting successful MD studies with O&G wastewaters, potential of surfactants and other organics to wet the membrane pores, and that MD still has yet to be fully utilized commercially in any sector. GE's pilot of a MVC-MD unit which is detailed in RPSEA project NORM Mitigation and Clean Water Recovery from Marcellus Produced Water showed that MVC-MD can be an effective brine concentrator in O&G (Silva et al., 2014).

3.0 MATERIALS AND METHODS

3.1 MATERIALS USED

3.1.1 Membranes Utilized

Flat sheet acrylic copolymer membranes with 0.2µm and 0.45µm pore sizes were selected as the primary membranes for this study. These Versapor® AC membranes (S80273 - Versapor-200R membrane, 0.2 µm, 8" x 10" sheet; S8027 - Versapor-450R membrane, 0.45 µm, 8" x 10" sheet) were purchased through Pall Corporation and are marketed for medical venting applications.

This particular membrane material was selected for a number of reasons. Presently, there is no documentation available in the literature to indicate that AC membranes have been utilized in MD research. However, these membranes have many of the same properties as PTFE, PP, and PVDF membranes plus a few more robust characteristics which are well suited for this particular MD application. The foremost being that these membranes have been treated with Pall's patented Repel™ process which yields a membrane that is both hydrophobic and oleophobic. Therefore, these membranes should be resistant to water, oils, and organic solvents, and the latter two would likely be present in flowback/produced water waste streams from the oil and gas industry. A technical assessment of produced water treatment technologies which was completed by the Colorado School of Mines in 2009 for RPSEA Project 07122-12, considered the current MD

membranes insufficient for rejecting compounds with higher volatility than water. It also remarked that residual surfactants from the hydraulic fracturing process would wet the membrane, resulting in membrane pore flooding which would adversely affect the ability of the membrane to keep the brine separated from the clean distillate. With AC membranes these concerns could be curtailed. The particular Versapor® AC membranes selected for this study are on non-woven nylon support which is advantageous for the flat sheet DCMD module constructed for this study because the membranes are durable and should be able to withstand harsh experimental operating conditions.

The AC flat sheet membranes employed in this study were characterized using scanning electron microcopy. Fig. 3 (a) and Fig. 4 (a) confirm that the membrane thickness for both 0.2µm and 0.45µm pore sizes is approximately 150µm, which is reasonable for MD applications. Reported membrane thickness for flat sheet MD operations typically fall between 25µm and 185µm while the average membrane thickness is roughly 110-120µm, (Khayet, 2011 and Alkhudhiri et al., 2012). The 0.45 and 0.2 µm pore sizes also fall within the typical range in MD studies (Adnan et al., 2012; Alkhudhiri et al., 2012). Pall Corporation states that these membranes are composed of two acrylic copolymer layers with the internal nylon support. Both sides of the membrane are active. By looking at Fig. 3 (b) and (c) as well as Fig. 4 (b) and (c), one can see that the two sides of the membrane have similar morphologies.

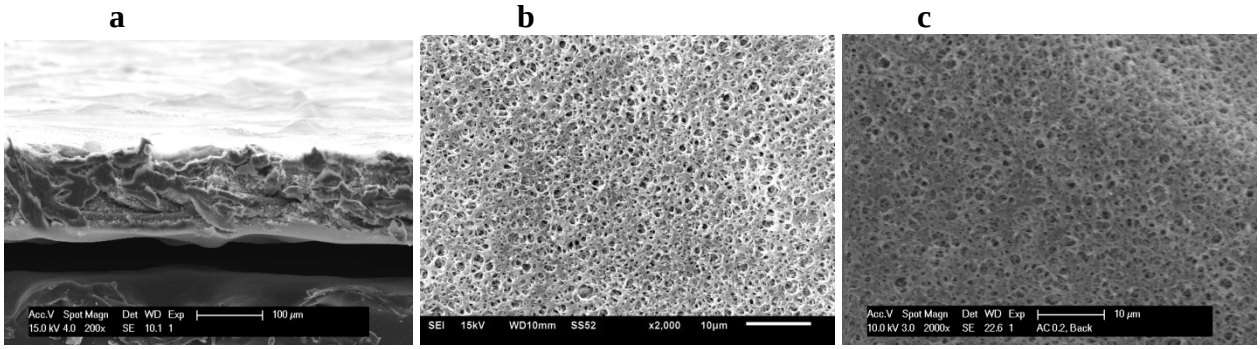

Figure 3. Scanning electron micropgraphs for 0.2µm AC flat sheet membrane: (a) side view, (b) top view and (c) bottom view.

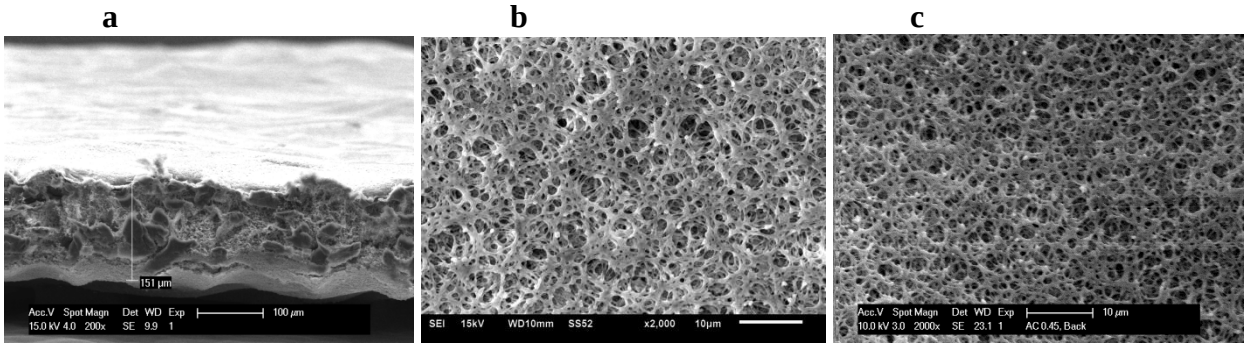

Figure 4. Scanning electron micropgraphs for 0.45µm AC flat sheet membrane: (a) side view, (b) top view and (c) bottom view.

The LEPw, which is the minimum pressure required to overcome the hydrophobicity and "wet" the membrane pores, was measured using the procedure describe in Section 3.3.6. The results were 410 and 340kPa for 0.2µm and 0.45µm AC flat sheet membranes, respectively. Khayet summarized reported LEPw values for flat sheet commercial membranes commonly used in MD applications to be between 48 to 463kPa with an average value of 230kPa (Khayet, 2011). The corresponding static water contact angle, which is a measure of the hydrophobicity of the membrane, was measured using the procedure describe in Section 3.3.5. The results were $143.3^{\circ} \pm 0.1$ and $138.75^{\circ} \pm 0.35$ for 0.2µm and 0.45µm membranes, respectively. For comparison

the water contact angle was 107˚ and 120˚ for PVDF and PP membranes used in a MD application (Curcio and Drioli, 2005) and 161˚ to 121˚ and 165˚ to 133˚ for 0.2µm and 0.45µm PTFE membranes respectively (Adnan et al., 2012). The static hexadecane contact angle, which is a measure of the oleophobicity of the membrane, was measured at 116.35˚ ± 0.35 and 115.95˚ ± 0.95 for 0.2µm and 0.45µm membranes, respectively.

3.1.2 Test Solutions

Characteristics of flowback and produced water from natural gas extraction vary greatly due to a number of factors; be it different shale plays, locations within a certain shale play, the length of time the water was in contact with the formation, and the quality of the source water used for hydraulic fracturing. Samples for this study were sourced from two well sites in the Marcellus Shale play in southwestern Pennsylvania.

3.1.2.1 Real Flowback and Produced Water Samples

Well site A is located in Westmoreland County and was hydraulically fractured in June 2010. The water used for hydraulic fracturing this well was sourced from a local municipal drinking water treatment plant. The producer initiated flowback within a few days of hydraulically fracturing the well so that the water did not remain in contact with the formation for an extended period of time. Grab samples were collected on the first, second, fourth, fifth, seventh, twelfth, and fifteenth day after flowback was initiated and all samples were collected before the well was completed and went into production. The TDS concentration of the daily grab samples increases

with time while the volume of water flowing back decreases as demonstrated in Figure 5. A flow-weighted composite sample of these waters was the primary water utilized in this MD investigation. This water will be referred to as A1.

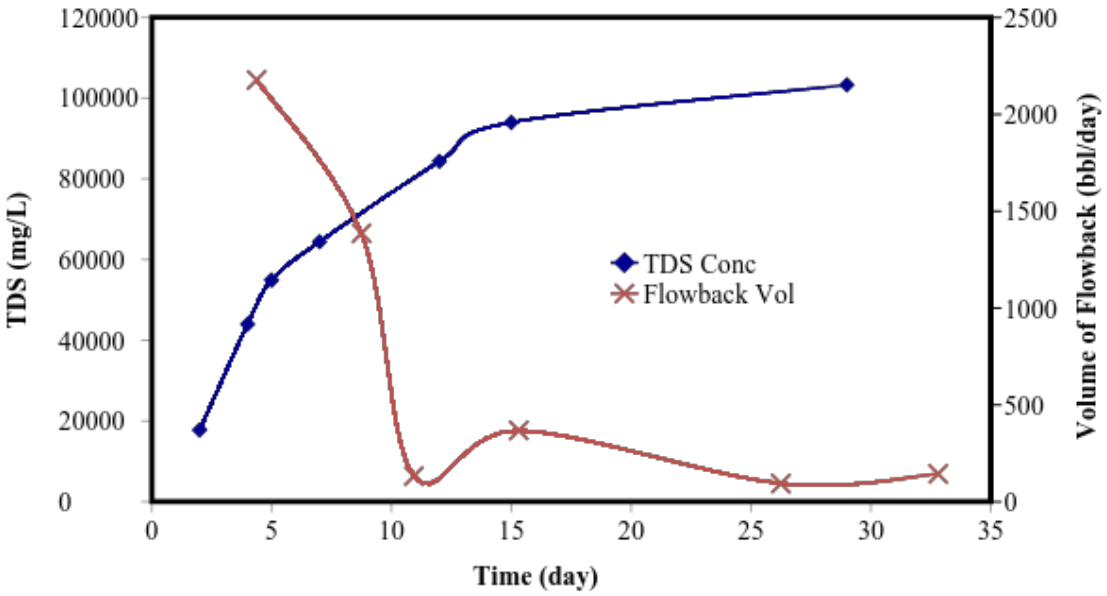

Figure 5. Site A's TDS concentration and volume versus time after flowback initiated.

A produced water sample was collected from Site A in July 2012, which is approximately 2 years after the well was hydraulically fractured. This water will be referred to as A2.

Well site B is located in Washington County and was hydraulically fractured in June 2010. The water used to hydraulically fracture the well was recycled flowback water. The recycle/reuse strategy has become the new industry standard in the Marcellus Shale play. The water at site B remained in contact with the formation for approximately 10 days before the producer initiated flowback. Samples were collected on the first, third, fifth, seventh, tenth, fifteenth, and twentieth days after flowback was initiated and before the well was completed and went into production. As with site A, the TDS concentration of the samples from site B increases

with time as the volume of water flowing back decreased. This water has not been heavily studied yet with this MD setup; however the water sample from Day 20 was used and shall be referred to as B1.

The main parameters characterizing these samples from unconventional gas extraction in Marcellus Shale formations are listed in Table 2.

Table 2. Flowback Water Characteristics

Constituent	A1	A2	B1
Na [mg/L]	16,518	NA	47,881
Ca [mg/L]	2,224	NA	18,080
Mg [mg/L]	220	NA	1,992
Ba [mg/L]	781	3,924	379
Sr [mg/L]	367	1,560	2,151
Cl [mg/L]	29,000	NA	112,471
TDS [%]	3.9	13.7	18.3

Well Site A water was selected over Well Site B water as the primary water utilized in this MD investigation because it has lower TDS concentration. This allows for more comparison based on TDS to existing studies in the literature, which are most frequently measuring seawater or RO concentrate and offered a wider range of possible TDS values to test.

All real water samples used in the study were filtered prior to use in the MD system to remove suspended solids. Whatman (0.45 μm Glass Microfibre, 934-AH) and Millipore (0.05 and 0.45 μm, Type VVLP) filters were utilized to remove suspended solids from raw water samples prior to all MD test runs.

3.1.2.2 Synthetic Flowback

A synthetic flowback water composition based on the water chemistry of A1 with a TDS of 3.9% was used for several experiments. Synthetic flowback sample was also concentrated 4,

6, and 7 times resulting in TDS values of 15.6%, 23.4%, and 27.3%. The base synthetic flowback sample will be referred to as SynA1 and is listed in Table 3.

Table 3. Synthetic A1 recipe with TDS of 3.9%

Salts	**Concentration (g/L)**
NaCl	30.148
$CaCl_2 \cdot 2\ H_2O$	8.116
$MgCl_2 \cdot 6\ H_2O$	1.839
$BaCl_2 \cdot 2\ H_2O$	1.389
$SrCl_2 \cdot 6\ H_2O$	1.116

Reagents used in this study were of analytical grade (Barium Chloride, Dihydrate, Assay 99.0% min, Mallinckrodt Chemicals; Strontium Chloride, Hexahydrate, Assay 99%, Acros Organics; Sodium Chloride, Assay 99.8%, Fisher Scientific; Magnesium Chloride, Hexahydrate, Assay 100.1%, J.T.Baker; Calcium Chloride, Dihydrate, Assay 99.0~105.0%, EMD). All synthetic waters were prepared by using de-ionized water (with a resistance of 17.8 MΩ).

3.2 EXPERIMENTAL SETUP

3.2.1 Experimental setup

A bench scale direct contact membrane distillation (DCMD) system was designed and built for this study. The hot feed side and the cold permeate side essentially mirror one another. Water was pumped from the reservoir (4 L Erlenmeyer flask feed side; 4 L Büchner flask permeate side) with a centrifugal pump (115 V March Pump, AC-3CP-MD) and was returned back to the reservoir after passing through the module. The water pressure was measured using a pressure gauge, (catalog no. 4FLT8, Grainger) and the flowrate was measured using a 0.2-2.5gpm

flowmeter, (catalog no. 5P321, Grainger). The water temperature was measured both immediately before and after it passes through the membrane module, (NSF certified Pocket Digital Thermometer, -40˚ to 450˚F, catalog no. 3009K42, McMaster-Carr). Both the hot feed and cold permeate sides have a bypass line with a ball valve to allow for a portion of the water to bypass the membrane module and return to the reservoir as a way to control the flowrate. The majority of the fittings are compression tube fittings (½ inch outer diameter, McMaster-Carr). The feed reservoir was heated on a hot plate (Fisher Scientific Isotemp). The permeate reservoir was partially submerged in a 12-gallon cold water bath. The temperature of the cold water bath was kept at 10˚C by recirculating water through a water chiller (NESLAB Thermo Scientific M75 Merlin Chiller) and then copper tubing in the water bath. To measure the permeate flux, a tube connected to the sidearm of the Büchner flask (permeate reservoir) which allowed the water to flow into a smaller container placed on a balance (OHAUS Navigator XT). A conductivity probe (Fisher Scientific accumet Excel XL25 pH/mV/Temperature/ISE Meter) was placed inside the permeate reservoir to ensure that there is no salt breakthrough as a result of membrane pore flooding during an experimental run. Figure 6 shows the experimental setup with the key elements of the bench scale system.

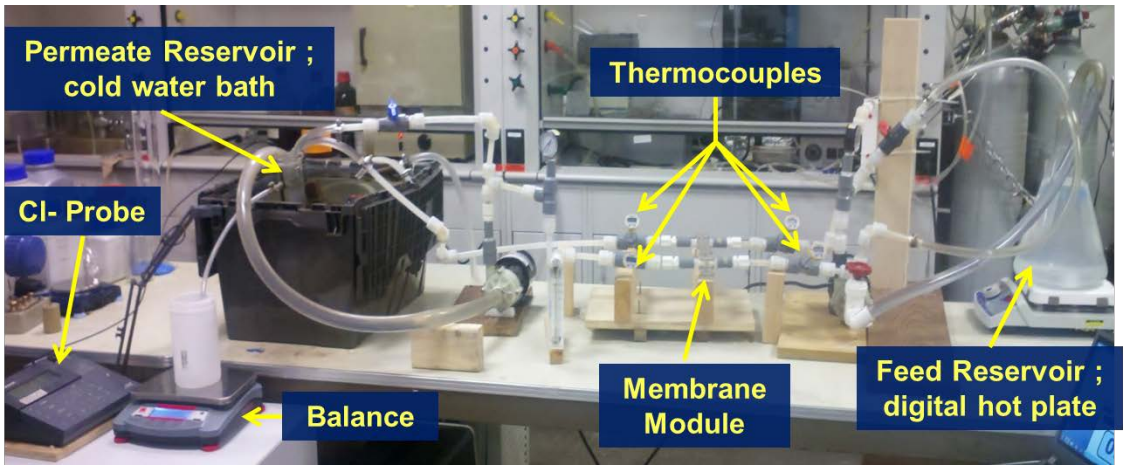

Figure 6. Picture of the DCMD bench scale system.

The system was designed to maximize flexibility in the setup and to allow for easy removal of the membrane module to change the membrane between experiments. All experiments in this study employed counter-current flow pattern of the feed and the permeate streams through the membrane module.

3.2.2 DCMD Membrane Module Description

The DCMD membrane module was constructed from two symmetrical, Plexiglas pieces which are screwed together with 12 screws to sandwich the membrane in place. Each side of the module had a rubber o-ring outside of the channel to prevent water leakage and to fix the membrane in place. Figure 7 shows the membrane module.

Figure 7. Membrane module (a) side view (b) alternative side view

The Plexiglas pieces have channels which are 200mm long, 20mm wide, and 3mm deep and the module was designed to provide 0.004m^2 of contact surface area between the hot feed water and the membrane, which is comparable to modules reported in the literature (Yun et al, 2006). Plexiglas was selected because it allows a visual observation of the membrane surface during experiments and its low thermal conductivity. The calculated Reynolds number in this

module for a 15% NaCl solution at 0.75gpm flowrate is 5,432, which means there is consistent turbulent flow. Therefore the effects from temperature and concentration polarizations should be minimized.

3.3 EXPERIMENTAL PROCEDURES

To adequately assess the capabilities of membrane distillation and AC membranes as a viable treatment option for flowback and produced waters associated with shale gas drilling, a number of different experiments were conducted. The majority of the experimental work was centered on measuring MD flux performance. However, several other experimental procedures were developed to focus specifically on the AC membranes performance and whether it could withstand the harsh chemistries of flowback and produced water.

This study investigated both a new MD membrane material and a new application of MD technology. Therefore, an experimental plan was developed meticulously to determine how the different parameters affected the flux performance. The first MD tests were completed with distilled water to verify the integrity (no water leaks) of the bench-scale system and to validate performance of the bench scale system. The initial bench scale DCMD tests were then followed by experiments with pure sodium chloride solutions at different TDS levels, synthetic flowback (SynA1) at varying TDS concentrations, and then with real flowback and produced water samples.

3.3.1 DCMD Testing Protocol

All DCMD experiments were conducted at an average flowrate of 0.75gpm (2.8LPM) and typically lasted between 45 minutes and 1.5 hours. The temperature of the permeate side was maintained between 12 and 22˚C. The temperature of the feed side was kept between 51 and 55˚C for all water vapor flux values reported. This feed temperature range was selected because it is a realistic range where waste heat could be utilize in an industrial setting.

Values for water vapor flux were only recorded when the system temperatures were in equilibrium for at least a 15 minute time period. The weight of permeate collected was recorded periodically, typically in two minute intervals. The flux was then experimentally determined using the following equation:

$$J = \frac{(w_2 - w_1)}{(t_2 - t_1)SA} \tag{7}$$

where, w_1 is the weight of the permeate collected by t_1 time, w_2 is the weight of the permeate collected by t_2 time, and SA is the membrane surface area in contact with the feed. Values for temperature difference reported were calculated by averaging the difference between the feed and permeate temperatures using the following equation:

$$Temperature\ Difference = \frac{(T_{f1} - T_{p2}) + (T_{f2} - T_{p1})}{2} \tag{8}$$

where, T_{f1} and T_{f2} are the measured feed temperatures in and out of the module and T_{p1} and T_{p2} are the measured permeate temperatures in and out of the module. The feed inlet temperature was measured against the permeate outlet temperature and vice a versa because of the feed and permeate flow through the module in opposite directions.

To maintain a constant feed concentration during experiments, for every 20mL of permeate collected, 20mL of distilled water would be added to the feed reservoir, (Adnan et al., 2012; Lawson and Lloyd, 1996).

A new membrane was used for each experiment unless otherwise noted. For all experiments conducted there were no signs of pore wetting and ionic breakthrough.

3.3.2 Module and Membrane Rinsing Protocols

The feed side of the membrane module was rinsed thoroughly after each experiment to ensure that residual feed would not dry and leave salt crystals in the system which could influence future experiments. First the majority of the feed water was drained from the system by disconnecting different sections of the system and then allowing water to drain by gravity. Different sections of system tubing, including sections that passed through the pump, pressure gauge, and thermometers were rinsed using tap water. The tap water rinse was followed with a rinse with 2 L of deionized water. Tap water was never run through the membrane module itself. After rinsing the module, the system was then reconnected to the module and 2 L of deionized water at ambient temperature was circulated through the system and module to rinse the membrane.

The effectiveness of the general rinsing procedure was measured following a 75 minute experiment with a 0.45 μm acrylic copolymer membrane treating synthetic A1 water (23.4% salt). After the system and module were rinsed, 3.5 L of deionized water was placed in the feed reservoir and cycled through the system at ambient temperature for 30 minutes at 0.8 gpm. The conductivity probe was used to measure the chloride level of the water in the feed reservoir and found that the changes were negligible (less than 1.5 mg/L fluctuation from the lowest

concentration and the highest concentration measured) during the 30 minute run time. Periodic rinsing with clean water in DCMD applications were also found effective in maintain membrane performance (Ngheim et al., 2011, Song et al., 2008).

After the rinsing protocol, the membranes were either removed from the module and saved for SEM/EDX analysis or the clean water permeability was measured to assess if there was notable flux performance degradation from the previous test.

3.3.3 SEM and EDX Analysis

The morphology of the membranes and any precipitates on the used membrane surface was inspected using Scanning Electron Microscopy (SEM, Philips XL30, FEI Co., Hillsboro, OR) and the elemental composition of selected samples was determined by Energy Dispersive X-ray Spectroscopy (EDS, EDAX Inc., Mahwah, NJ).

3.3.4 Membrane Longevity Testing

Due to the complexity of the wastewater evaluated in this study and the fact that the acrylic copolymer membrane has not previously been investigated for MD applications, it was necessary to evaluate the long-term performance of this membrane. The bench scale DCMD system designed for this study is not capable of performing a long-term experiment and it was decided to expose membrane samples to the feed solution for a long time and assess key characteristics of the membrane to determine possible degradation of the membrane material.

AC membrane samples were cut to 13mm diameter circles and were floated on top of the feed liquid in 400mL beakers covered with parafilm to prevent evaporation. The beakers were

partially submerged in a water bath that was controlled at 50°C. Only one side of the membrane was in contact with the feed solution. The beakers were rotated approximately one time every three days so that they would be evenly heated. Each beaker had four membrane samples floating on 350mL of A2 (produced water). Four membrane samples of each pore size were collected after 1 week, 2 weeks, and 4 weeks of exposure to A2 fluid. Two membrane samples of each pore size were used to measure the water contact angles and two membranes samples were used to measure the LEP_w to determine possible changes in hydrophobic properties. Figure 8 shows the setup for this test.

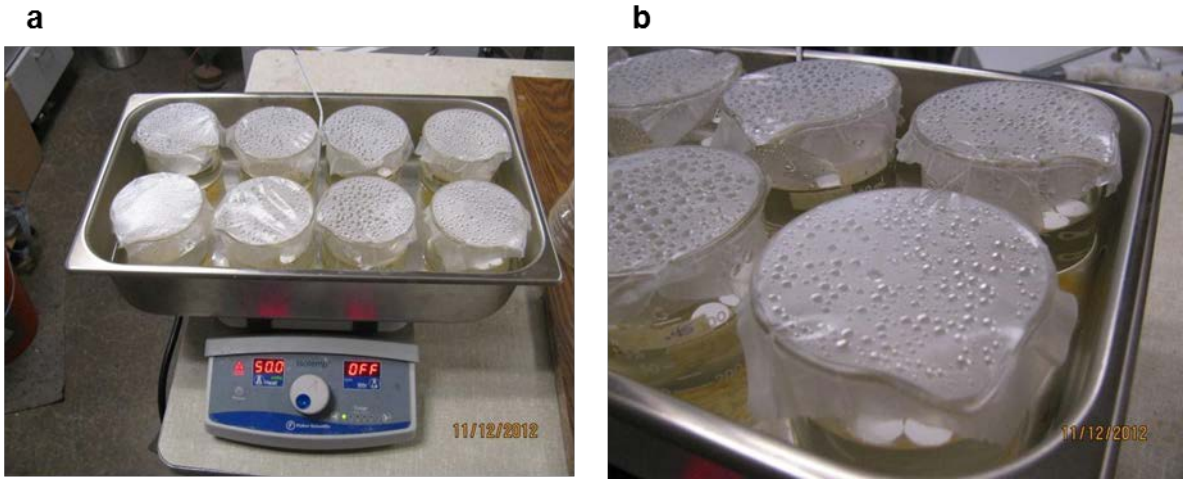

Figure 8. Membrane floating set-up

3.3.5 Measuring the Contact Angle

The water and hexadecane contact angles were measured using a VCA-OPTIMA drop shape analysis system (AST Products, Inc., Billerica, MA) with a computer-controlled liquid dispensing system. A built in image system would acquire the image, transmit to a computer and perform the analysis. The static water contact angles were measured with droplets that had a volume of 3µL. The advancing contact angles were recorded while the droplet sizes were

expanded by placing a needle in the water droplets and continuously supplying water through the needle. Each measurement was repeated three times. The measurements were performed under normal laboratory ambient conditions (20˚C and 30% relative humidity).

3.3.6 Determining the LEP_w

The industry-wide accepted methodology for measuring the liquid-entry-pressure of water, LEP_w, was established by Smolders and Franken (1989) and is the basis for the method utilized in this work. The apparatus described in Smolders and Franken (1989) which was replicated and used for determining LEP_w is show in Figure 9.

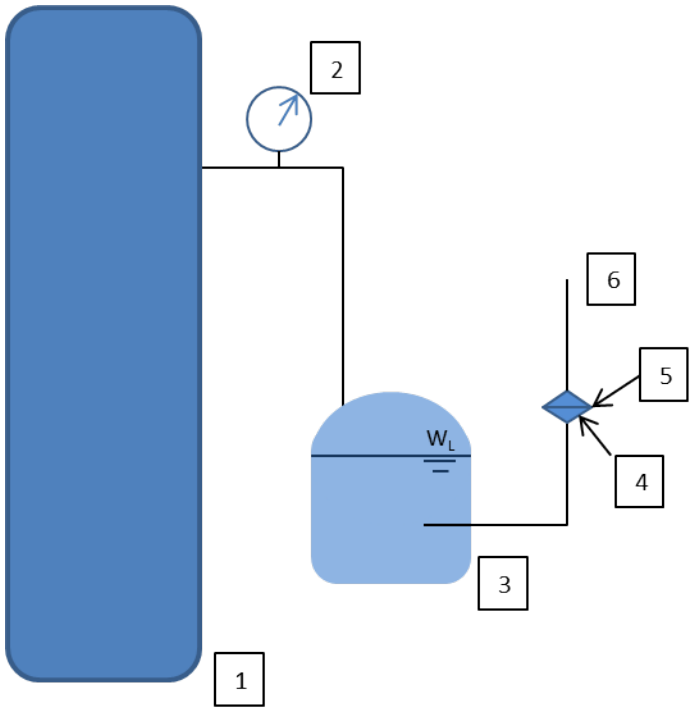

Figure 9. Apparatus for determining liquid-entry-pressure, LEPw. 1 - nitrogen gas cylinder; 2 - pressure gauge; 3 - liquid feed pressure vessel; 4 - measuring cell (filter holder); 5 - membrane; 6 - capillary tube.

To set up the test, a membrane sample was placed into the measuring cell/filter holder (EMD Millipore Swinnex™ Filter Holder, Dia.: 13mm, catalog no. SX0001301, Fisher Scientific). The liquid feed pressure vessel, the measuring cell, the tubing between the two, and the measuring tube are filled with distilled water. A slight pressure is applied to the system, (approximately 200 kPa), using the nitrogen gas cylinder to degasify the tubing and the measuring cell. Once the gas bubbles stop appearing in the capillary tube, the system is degasified and ready to measure the LEP_w of the membrane.

To measure the LEP_w of the membrane samples, the pressure is raised stepwise (10 kPa per step; 2 minutes per step) and the capillary tube is observed to see whether a flux through the membrane occurs. Once a continuous flux is observed, the LEP_w is reached as defined in section 2.2.2.1.

4.0 RESULTS AND DISCUSSION

4.1 MD WITH DIFFERENT FEED WATERS

4.1.1 Preliminary Studies with Sodium Chloride Solutions

Before testing the feasibility of MD as a final treatment method for flowback/produced waters from the Marcellus Shale with AC membranes it was important to establish the stability of the DCMD module and ensure that there is adequate flux performance through the AC membrane. Preliminary measurements with sodium chloride solutions were carried out and compared to flux performance in the literature as shown in Table 4.

Table 4. AC Membrane Performance Compared with References

Membrane Properties		Experiment Details					Flux (kg/m^2hr)	Source
Material	Pore Size, µm	Feed Flowrate	Feed Solution	T_f, °C	T_p, °C	T Dif, °C		
AC	0.45	0.75 gpm	3.5% NaCl	54	20	34	30.1	This study
AC	0.45	0.75 gpm	10% NaCl	55	21	34	25.8	This study
AC	0.45	0.75 gpm	20% NaCl	54	20	34	17.3	This study
AC	0.45	0.75 gpm	30% NaCl	54	20	34	9	This study
PTFE	0.03	500 mL/min	1% NaCl	85	20	65	14.5	Singh and Sirkar, 2012
PVDF	0.2	0.145 m/s	Distilled Water	50	19.7	30.3	14.4	Yun et al., 2006
PVDF	0.2	0.145 m/s	17.76% NaCl	50	20.5	29.5	9.9	Yun et al., 2006
PTFE	0.2	0.6 L/min	0.5% NaCl	50	20	30	27	Adnan et al., 2012
PTFE	0.45	0.6 L/min	0.5% NaCl	50	20	30	36	Adnan et al., 2012
PVDF	0.4	0.9 m/s	Distilled Water	60	21	39	30	Schofield et al., 1990
PVDF	0.4	0.9 m/s	14% NaCl	60	21	39	25	Schofield et al., 1990
PVDF	0.4	0.9 m/s	25% NaCl	60	21	39	21	Schofield et al., 1990
PVDF	0.2	0.53 m/s	2M Na2SO4	60	20	40	22	Tun et al., 2005
PVDF	0.2	0.53 m/s	4.5 M NaCl	60	20	40	21	Tun et al., 2005
PTFE	0.2	1.75 m/s	0.6 g/L NaCl	50	20	30	45	Cath et al., 2004
PTFE	0.45	1.75 m/s	0.6 g/L NaCl	50	20	30	52	Cath et al., 2004
PTFE	n/a	500 mL/min	3.5% NaCl	60	20	40	27	Silva et al., 2014

The data presented in Table 4 indicate that AC membrane performance is comparable to the other hydrophobic membranes which have been widely accepted by the MD industry during short-term experiments. The measured flux values with AC membranes are consistent, and in several instances even better when compared to other values reported in the literature. These results suggest that AC membranes and the experimental setup/module developed in this study are suitable for DCMD testing.

4.1.2 Studies with Sodium Chloride Solution and Synthetic Flowback

Because the majority of experiments conducted with membrane distillation in the literature have been completed with pure sodium chloride solutions, a crucial element in this study was to test whether any of the major ions commonly found in flowback affect the performance of DCMD

when compared to tests measured with pure sodium chloride solutions. The first flowback water DCMD experiments were conducted with SynA1 water and were then compared to the pure sodium chloride solution as shown in Figure 10.

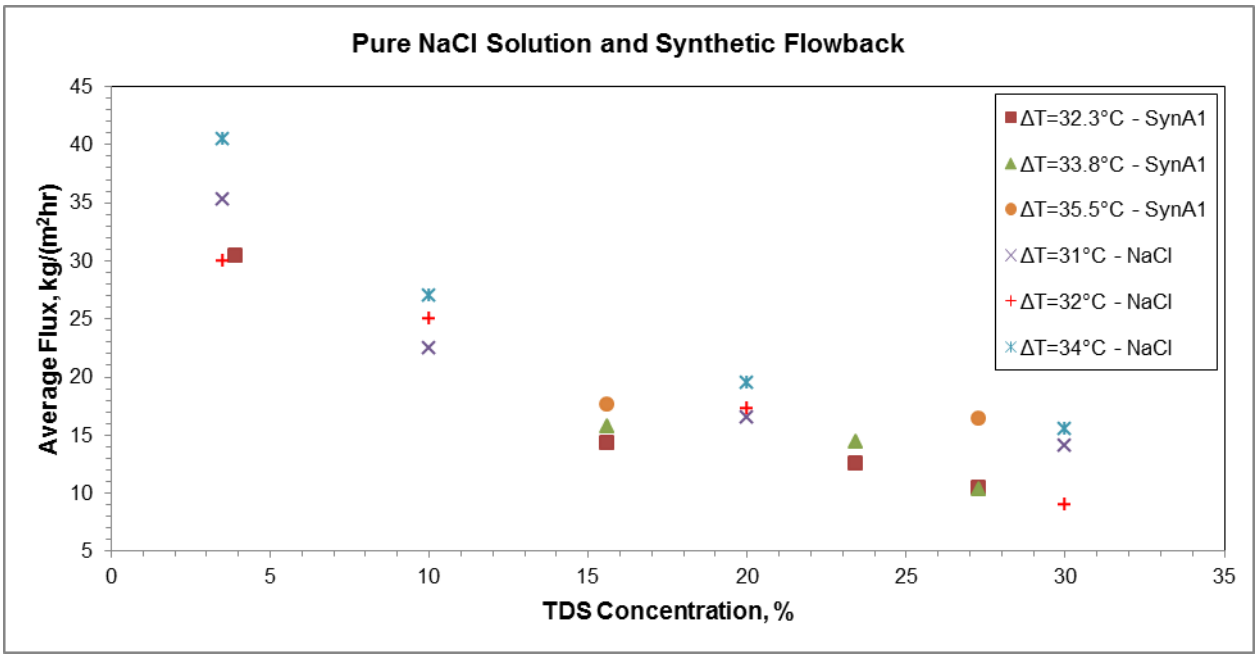

Figure 10. Comparison of Permeate Flux with Pure NaCl Solution and Synthetic Flowback

The results shown in Figure 10 were obtained using acrylic copolymer membrane with 0.45µm pore size. All data points had an average feed inlet temperature of 54.4°C to 55.3°C (averaged at 54.5°C) when the average flux measurement was recorded. Permeate flux increased with an increase in temperature difference between the feed and permeate sides for a given TDS.

Generally speaking there is little difference between the permeate flux measured using pure sodium chloride and synthetic flowback water for all TDS values tested in this study. The permeate flux decreased as the TDS concentration increased for both pure sodium chloride and synthetic flowback waters. This trend is asymptotic as the decrease in permeate flux is dramatic at first and then it relatively stabilizes when TDS of the feed was above 15%. Two other MD

studies have reported similar trends where the salinity increase resulted in flux decrease, which became more gradual once the salinity reached 13-15%, (Ji et al., 2010; Walton et al., 2004). A study on the effect of salinity on water evaporation found that there was initially a negative deviation from Raoult's law with salinity increase followed by a positive deviation from Raoult's law as the solution approached 30% (Panin and Brezgunov, 2007). The measured average flux versus salinity as shown in Figure 10 appears to follow a similar trend.

The data shown in Figure 10 suggest that the permeate flux is only slightly impacted by the replacement of monovalent Na^{+} cations with divalent cations (i.e., Mg^{+2}, Ca^{+2}, Sr^{+2}, and Ba^{+2}) in the synthetic solution, which is in line with fundamentals of MD. As the increase in temperature difference increases permeate flux by increasing the vapor pressure (i.e., the driving force), replacing monovalent Na^{+} cations with divalent cations decreases the mole fraction of the water in solution which would decrease the vapor pressure according to Raoult's law. Even though 77% of the cations by weight is attributed to Na^{+} ions in the SynA1 recipe, the effect of the divalent cations in the solution increases the mole faction of the solvents by 19% compared to pure NaCl solution, which is enough to cause a slight decrease in vapor pressure (0.3%).

4.1.3 Studies with Synthetic and Actual Flowback

Following DCMD performance comparison using synthetic flowback and pure sodium chloride solutions, the next step was to compare those results with actual flowback water tests to see if any of the incidental ionic compounds or any potential residual oils and organic solvents found in the actual flowback could affect the results.

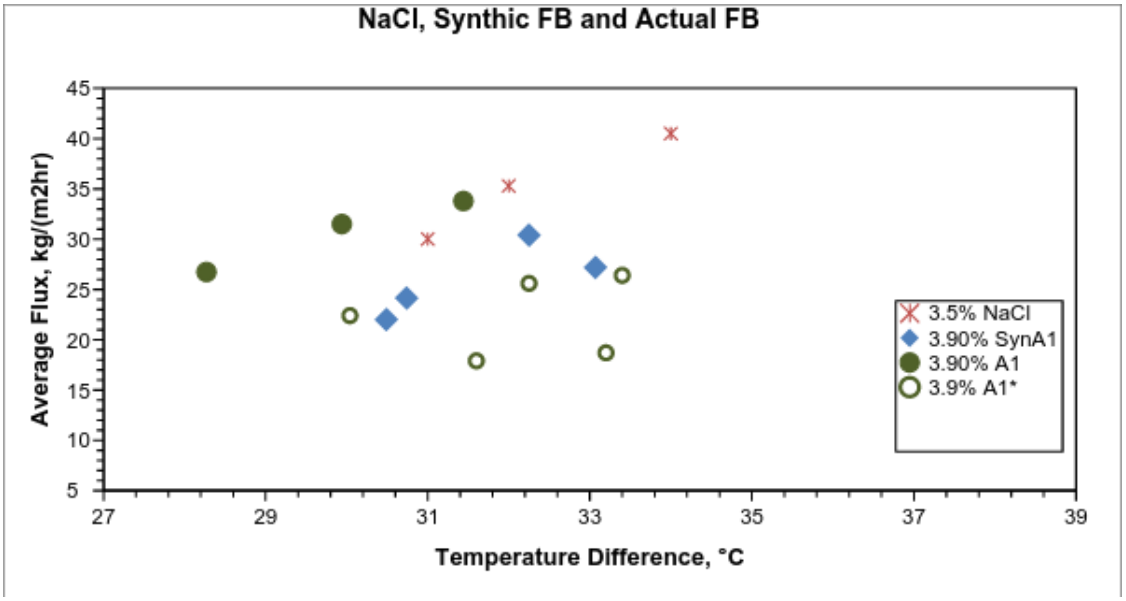

Figure 11. Permeate Flux for NaCl, Synthetic and Actual Flowback

The results shown in Figure 11 were obtained using acrylic copolymer 0.45µm pore size membranes. The percent reported in the legend for each data set is the percent TDS in the feed solution. The average feed inlet temperature when the average flux measurement was recorded was approximately 55°C for NaCl, 53.7°C for SynA1, 51.8°C for A1, and 52.6°C for A1* data sets. The permeate temperature was between 18.7°C and 22.5°C. Both A1 and A1* tests were completed with actual flowback but the A1* data set was obtained from experiments conducted 9 months after the A1 results.

Figure 11 shows that both sets of experiments conducted with actual flowback waters correlate well with the preexisting data generated from pure sodium chloride and synthetic flowback water experiments. The first set of experiments conducted with actual flowback (3.9% A1 in Figure 11) agrees well with pure sodium chloride flux results while the second set of experiments conducted with actual flowback (3.9% A1* in Figure 11) correlates with the

synthetic flowback flux results. These results are promising in that the actual flowback water yielded permeate flux that is comparable with that obtained with pure sodium chloride and synthetic water.

However, the difference in permeate flux between the two sets of experiments with A1 water is contradictory because the test results A1* had a higher average feed temperature but poorer flux performance then with A1. One possible explanation is that the experimental run with A1 had a feed flowrate of 0.85gpm while that used in tests with A1* was 0.7gpm. In their review of published literature, Alklaibi and Lior found that increasing the flowrate by 3-fold increases the flux by roughly 1.3-fold (2004).

The most critical takeaway from Figure 11 is that there is no glaring evidence that any oils or organics in actual flowback water wetted the acrylic copolymer membrane pores during testing because there was no significant increase in the permeate flux compared to that obtained with pure sodium chloride and SynA1 feeds. Also an increased chloride concentration in the permeate reservoir would have also been detected if the membrane pores had been wetted. While this does offer some verification to the durability and oleophobic properties of this particular acrylic copolymer membrane, the residual oil and organic concentrations were not measured in the actual flowback and the tests with actual flowback did not exceed two hours.

4.1.4 Studies with Different Actual Waters

The majority of the results in this study were obtained using flowback water from Well Site A located in Westmoreland county, PA. To confirm that the relatively high flux was not just achievable for this one flowback with a fairly low TDS, other actual Marcellus Shale water samples were tested in the DCMD system. These samples were produced water from Well Site A

(A2) and flowback water from Well Site B (B1) which is in Washington county, PA. Figure 12 compares the permeate flux obtained from A1, A2 and B1 flowback and produced waters. Figure 13 compares the permeate flux obtained from A2 and B1 flowback and produced waters to the permeate flux obtained with high salt synthetic flowback water.

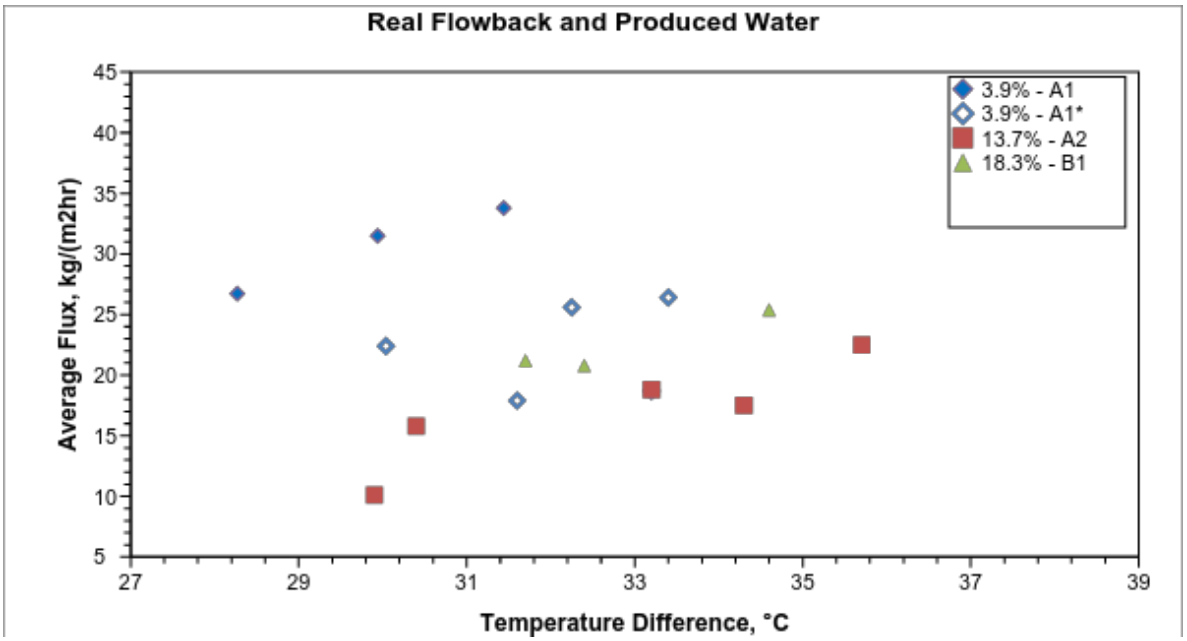

Figure 12. Permeate Flux for Actual Flowback and Produced Water

The results shown in Figure 12 were obtained using acrylic copolymer 0.45µm pore size membranes. The percent reported in the legend for each data set is the percent TDS of the test water. The average feed inlet temperature when the average flux measurement was recorded was approximately 51.8°C for A1, 52.6°C for A1*, 52.8°C for A2, and 54.5°C for B1 data set.

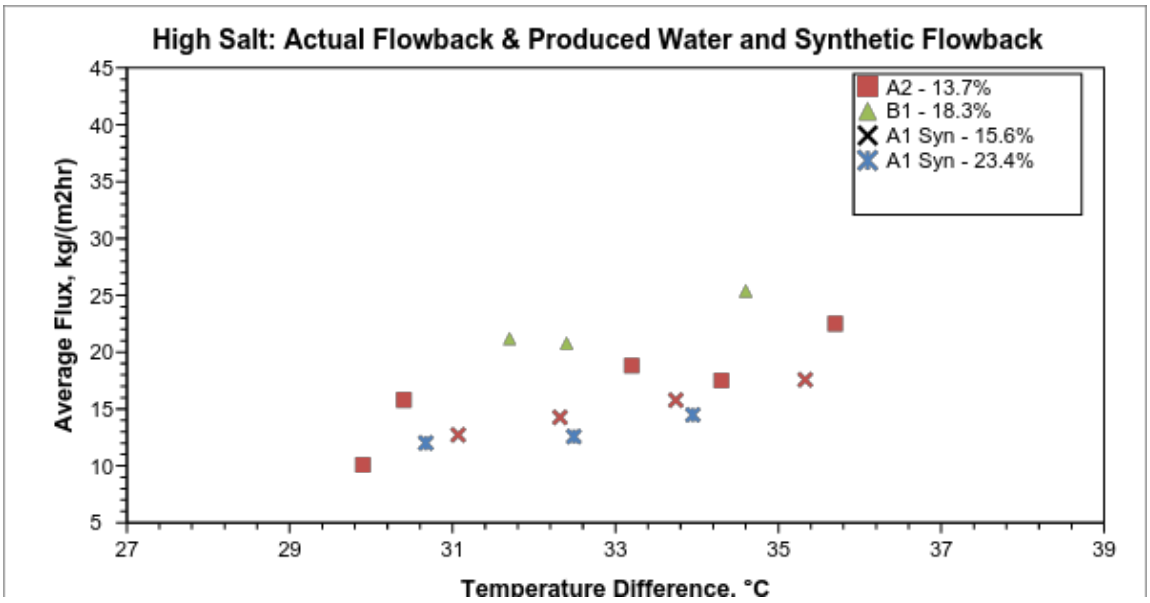

Figure 13. Permeate Flux for Actual Flowback and Produced Waters and High Salinity Synthetic Flowback

The results shown in Figure 13 were obtained using acrylic copolymer 0.45µm pore size membranes. The percent reported in the legend for each data set is the percent TDS of the test water. The average feed inlet temperature when the average flux measurement was recorded was approximately 52.8°C for A2, 54.5°C for B1, and 54.2°C for 15.6% Syn A1, and 53.7°C for 23.4% Syn A1 data sets.

As with the pure NaCl, Synthetic A1, and Actual A1 waters, the permeate flux for both A2 and B1 generally improves as the temperature difference increases (increase in the driving potential) as seen in Figures 12 and 13. Similar flux performance found between A2 and B1 (and compared to the synthetic A1 flux performance in Figure 13), correlates well with the conclusion drawn from Figure 10, which showed that the permeate flux stabilizes at roughly 15% salt since the permeate fluxes measured do not vary greatly even though the percent TDS varies from 13.7% to 23.4%. However, the B1 flux was higher than A2 flux despite B1 having the higher salinity. This could be explained by another study where there was severe pore blockage and

membrane fouling with A1 waters and not with B1 waters in a dead end microfiltration application (He, 2014). Although membrane fouling wasn't observed on the membranes used in A1 and A2 testing with SEM analysis, there could be some slight effect not identified with SEM analysis.

The results shown in Figure 13 do not have any indication that residual oils or organics in the actual flowback or produced waters wetted the acrylic copolymer membrane pores during this testing. This correlates with what was discussed in Section 4.1.3.

4.2 IMPACT OF MEMBRANE PORE SIZE ON DCMD PERFORMANCE

The effect of membrane pore size on the performance of DCMD system with these complex wastewaters was investigated in this study. "The importance of membrane pore size on DCMD performance has not been studied widely compared to porosity and thickness suggesting that it is less important for flux improvement," (Adnan et al., 2012). However, when selecting a membrane pore size for MD applications, on must weigh whether high production rates or distillate quality is more important for that particular application. Smaller membrane pore size typically results in higher LEPs and lower production rates, (Khayet, 2011). As stated in Section 3.3.1, for all experiments conducted in this study, there were no signs of pore wetting and ionic breakthrough or reportable increases in the conductivity of the permeate. Thus performance based comparison is the best way to compare the membranes with different pore sizes. This was done by comparing the permeate flux and scaling potential/rinsing effectiveness of 0.2 and 0.45 µm pore size AC membranes.

4.2.1 Permeate Flux

Experiments with synthetic A1 solution at varying feed concentrations were used to study the impact of pore size on permeate flux. The permeate flux was measured as a function of temperature difference and the results are shown on Figure 14.

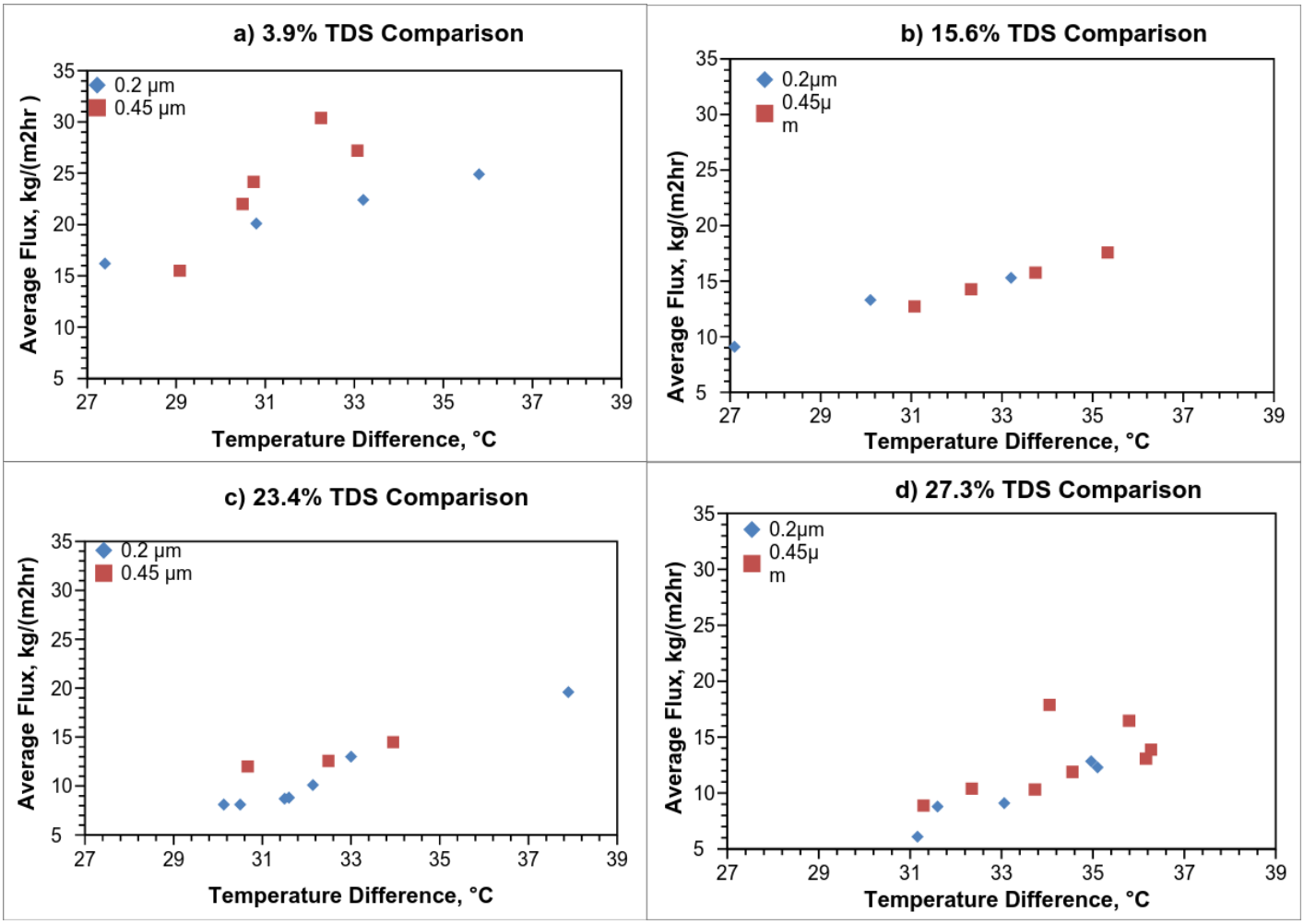

Figure 14. Permeate Flux as a Function of Temperature Difference for 0.2 and 0.45 µm AC membranes at different feed salinities

The results shown in Figure 14 were all measured during experiments with acrylic copolymer 0.2 and 0.45 µm pore size membranes as indicated. Table 5, details the average feed inlet temperature when the average flux measurement was recorded for the data reported in Figure 14.

Table 5. Figure 14 Operating Conditions

Figure Subpart	0.2 µm results Average Feed Temp, °C	0.45 µm results Average Feed Temp, °C
a) 3.9% TDS	54.2	53.7
b) 15.6% TDS	51.1	54.3
c) 23.4% TDS	53.8	53.7
d) 27.3% TDS	53.9	53.9

Figure 14 indicates that 0.45 µm membrane exhibited slightly better performance compared to 0.2 µm membranes as expected. The results shown in Figure 14 b are a bit surprising because the measured flux was almost identical for both 0.2 and 0.45µm AC membranes despite the difference in pore size and a 3.2°C higher average feed inlet temperature for the 0.45µm AC membrane. This is counterintuitive according to the heat and mass transfer theory of MD, which is discussed in Section 2. Adnan et al (2012), compared the performance of 0.2 and 0.45 µm pore sized PTFE membranes under identical operating parameters and found that 0.45µm pore size had slightly higher permeate flux but in general, the permeate flux does not differ greatly between 0.2 and 0.45µm pore sized membranes unless the feed temperature goes over 50°C. They attributed the growing difference in flux to higher temperature polarization for the 0.2 pore size membrane while the temperature polarization approaches 1 at higher feed temperatures, (Adnan et al., 2012).

4.2.2 Membrane Scaling/Cleaning

The rinsing procedure discussed in Section 3.3.2 was primarily developed for this study to prevent cross contamination and to prevent salt from crystallizing in the system's feed side tubing between experiments. It also offers insight into the effectiveness of AC membranes for long-term DCMD application for O&G wastewater treatment. The ability to easily clean the membrane to restore permeate flux means that routine CAPEX costs should be lower and make the process and that particular membrane more attractive for industrial applications.

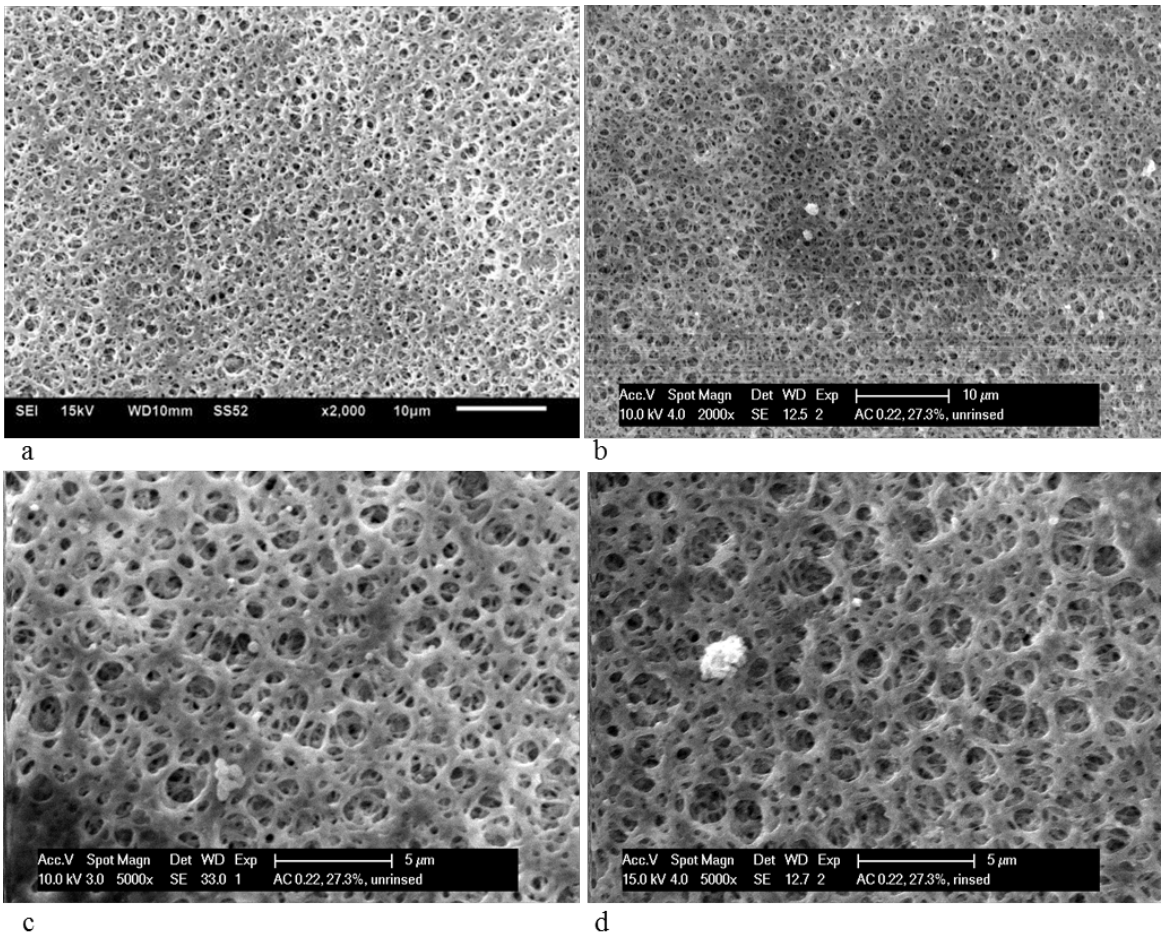

Figure 15. SEM images of 0.2 µm membranes: a) pristine membrane; b) and c) membrane used in test with synthetic flowback; d) membrane used in test with synthetic flowback after backwashing

Figure 15 a shows the SEM image of an unused 0.2 µm membrane. Figure 15 b and c show the SEM images of a used unrinsed 0.2 µm membrane sample from experiment conducted with concentrated synthetic flowback (27.3% TDS). The experimental runtime was 65 min and the EDX analysis identified the crystals as a mix of NaCl and $BaCl_2$. Figure 15 d shows the SEM image of a 0.2 µm membrane sample was collected after rinsing a membrane which was used for a 100 min long experiment with concentrated synthetic flowback (27.3% TDS). What appeared to be a crystal on the membrane surface in 15 d is likely an abnormality on the membrane surface since the EDX8 analysis only identified C, Si, Cl, O, S, and Pd elements. No NaCl or $BaCl_2$ crystals were identified on the rinsed membrane sample via SEM/EDX analysis.

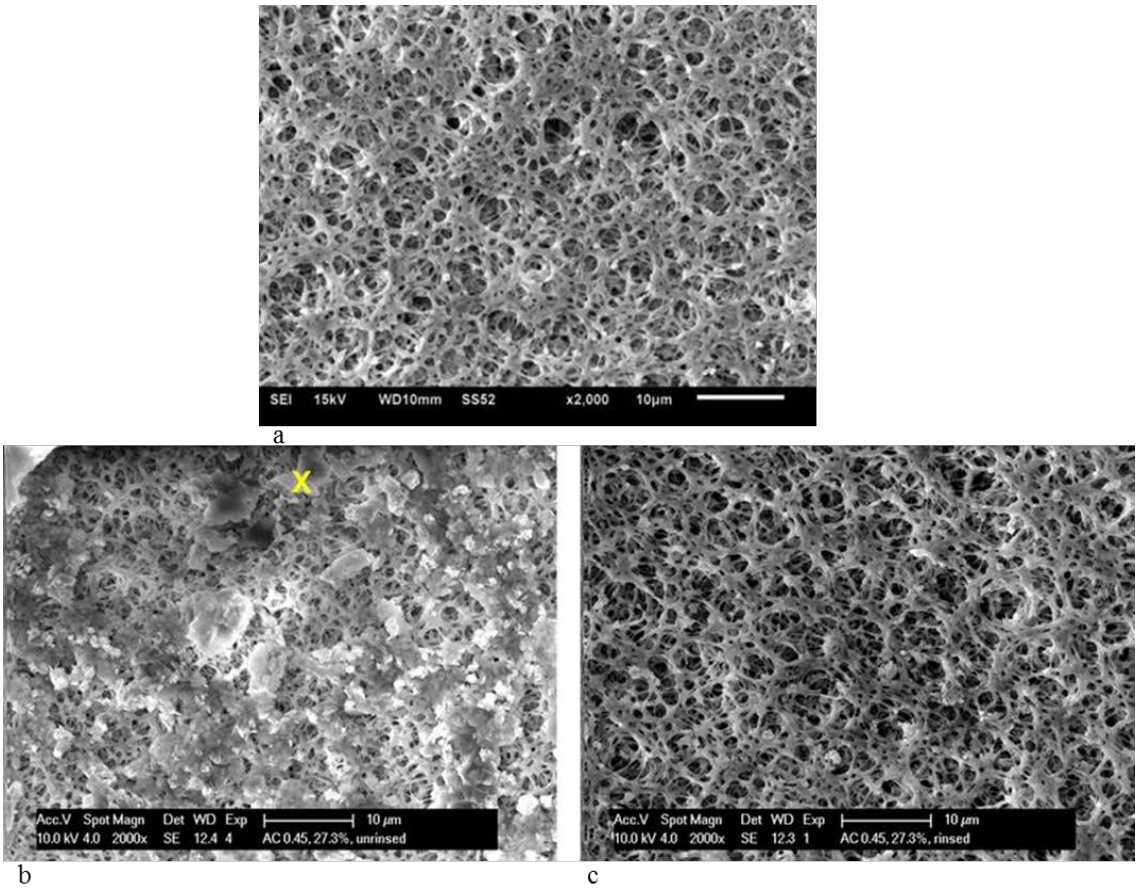

Figure 16. SEM images of 0.45 µm membranes: a) pristine membrane; b) membrane used in test with synthetic flowback; c) membrane used in test with synthetic flowback after backwashing

Figure 16 a shows the SEM image of an unused 0.45 µm membrane. Figure 16 b shows the SEM images of the 0.45 µm membrane used in the experiment with concentrated synthetic flowback (27.3% TDS) after 65 min. EDX analysis identified that the cake observed immediately on the membrane surface was primarily NaCl, the large salt crystal marked by X was BaCl2 and the smaller crystals were identified as a mixture of NaCl and BaCl2. Figure 16 c shows the SEM image of 0.45 µm membrane sample used for a 100 min long experiment with concentrated synthetic flowback (27.3% TDS) after rinsing. The salt crystals were identified as a mix of NaCl and $BaCl_2$ by EDX analysis.

Even though Ba concentration was typically lower than that of Ca and Mg in the synthetic A1 water it is expected that barium chloride would be far more prevalent on the membrane surface than calcium or magnesium chlorides because it's solubility in water is significantly lower (35.74 g/100 mL (20 °C) for $BaCl_2$, 72.80 g/100 mL (20 °C) for $CaCl_2$, and 55.23 g/100 mL (20 °C) for $MgCl_2$) (Clynne and Potter, 1979).

Figures 15 and 16 clearly indicate that the 0.45 µm membrane has a higher affinity towards scaling than the 0.2 µm membrane, which is likely due to greater surface roughness of the 0.45 µm membrane as shown on Figure 4. The difference in scaling behavior for the two membranes support the trends shown in Figure 14, where the permeate flux at higher concentrations did not vary greatly for 0.45 and 0.2 µm membranes, even though larger membrane pores should theoretically result in a higher permeate flux. It is likely that excess scaling on the 0.45 µm membrane at higher TDS inhibited mass transfer by blocking membrane pores leading to lower permeate flux that more closely matches that of the 0.2 µm membrane.

4.3 MEMBRANE LONGEVITY TESTING

To prove that AC membranes are indeed suitable for treatment with flowback and produced water the longevity of MD membranes is assessed by the stability of the membrane performance over time. This can include prominent and measurable results such as maintained flux performances and whether the membranes selectiveness and ability to maintain a certain degree of distillate quality over time is achieved. With the DCMD system designed and used in this study, true membrane longevity testing was not possible, but the following sections describe the results of experiments which offer some indication of the longevity of AC membranes in DCMD treatment of Marcellus flowback and produced water treatment.

4.3.1 Long Run Experiments

A crucial aspect of any membrane process is the longevity of the membrane under relevant operating conditions. This includes whether the membrane can sustain a consistent flux, the ability of the membrane to withstand cleaning, maintain distillate quality and then ultimately the membrane's usable lifespan. While the extended testing was not possible with this unit, it was still important to analyze the flux versus the temperature difference (the driving force) for a single run to see if there would be any notable flux decline during that period. Some of the longest tests in this study were 100 minutes and two of them are shown in Figures 17 and 18.

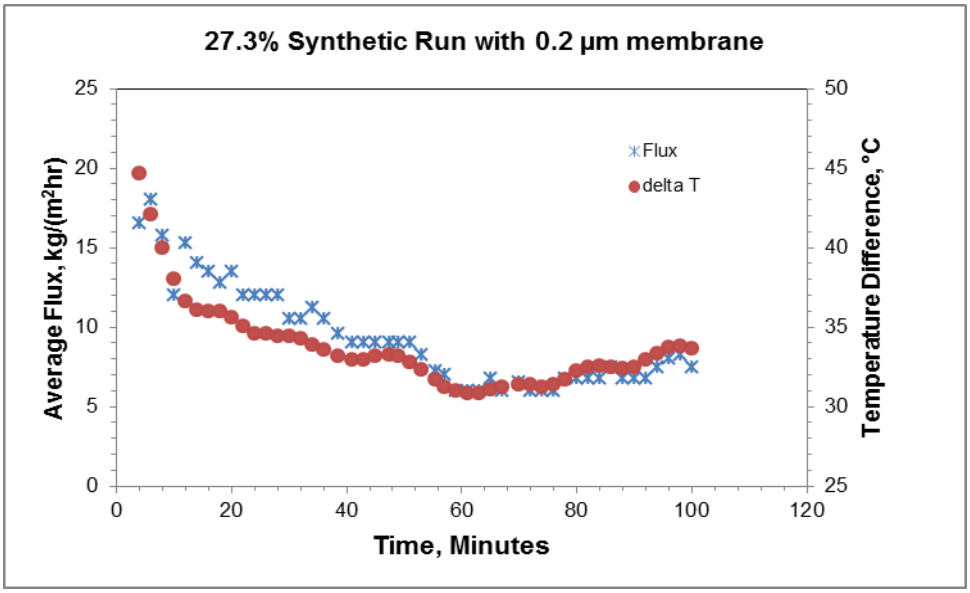

Figure 17. Membrane flux and temperature difference over time for 0.2 µm treating synthetic feed with 27.3% TDS

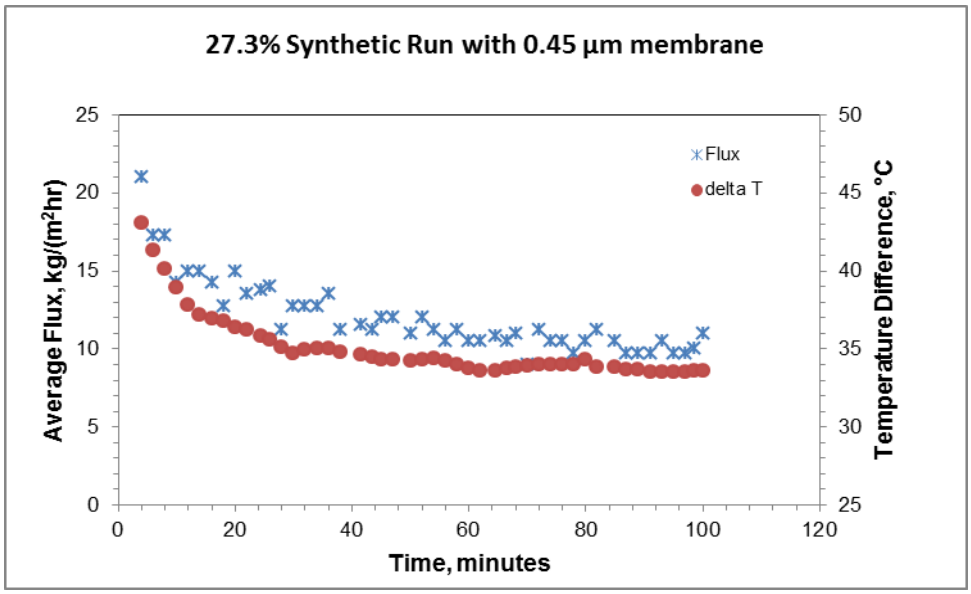

Figure 18. Membrane flux and temperature difference over time for 0.45 µm treating synthetic feed with 27.3% TDS

These runs with 27.3% synthetic A1 feed showed that the flux rate was not significantly degraded. Overall, the flux production followed the temperature difference profiles showing the

direct correlation between flux achieved and vapor pressure difference (brought on by the temperature difference). During the experiment detailed in Figure 17, the temperature profile was varied but the temperature difference was at 33°C at both 40 minutes and 90 minutes into the experiment run. The permeate flux however did not fully recover at the 90 minute mark and was 10% lower than at the 40 minute mark despite the average feed inlet temperature being 1°C higher at the 90 minute mark. In Figure 18, the temperature difference was maintained at an average of 34.1°C for 72 minutes, during which the flux production remained at a relatively consistent average of 10.9 kg/(m^2hr).

While an experiment lasting much longer would be more relevant, these initial tests are still promising, especially since the feed was nearly at halite saturation with a TDS of 27.3%. The results presented here are even more promising because the clean water flux of membranes used in long experiments was very close to that of the pristine membranes after rinsing. For example a membrane used in 120 minute test with 3.9% synthetic A1 feed exhibited clean water flux of 30.1 kg/(m^2hr) prior to the test and 29.6 kg/(m^2hr) after the test. Membrane used in the test depicted in Figure 17 had clean water flux at 30.6 kg/(m^2hr) prior to the test and 30.2 kg/(m^2hr) after. This agrees with the reports that membrane cleaning could recover permeability after long run experiments (Nghiem and Cath, 2011; Silva et al., 2014; Gryta, 2008).

4.3.2 Membrane Floating

As discussed in section 3.3.4, AC membrane samples, were contacted with ("floated" on) A2 water to simulate conditions that the membranes would be under in a long term DCMD operation to evaluate the longevity of AC membranes for treatment of oil and gas wastewater. Membrane samples were then collected after 1, 2, and 4 weeks of contact and the water contact angles and

LEPs were measured to assess the key characteristics of the membrane time over and to determine if there is any degradation of the membrane material. If there was significant membrane degradation after it had been in contact with produced water under simulated DCMD conditions, the full scale operations could require frequent membrane replacement to maintain produced water quality and likely render MD with AC membranes cost prohibitive for this particular application.

4.3.2.1 Water Contact Angle

The static and advancing contact angles were measured for AC membrane samples after long term exposure to produced water to see if any residual surfactants or organics would degrade the hydrophobic properties of this membrane. The contact angle measurements for membrane samples that were exposed to produced water for 1, 2 and 4 weeks are presented in Figures 19 and 20. For reference, contact angles of fresh membranes are also presented. All results presented are averaged from at least three independent contact angle measurements for each membrane sample.

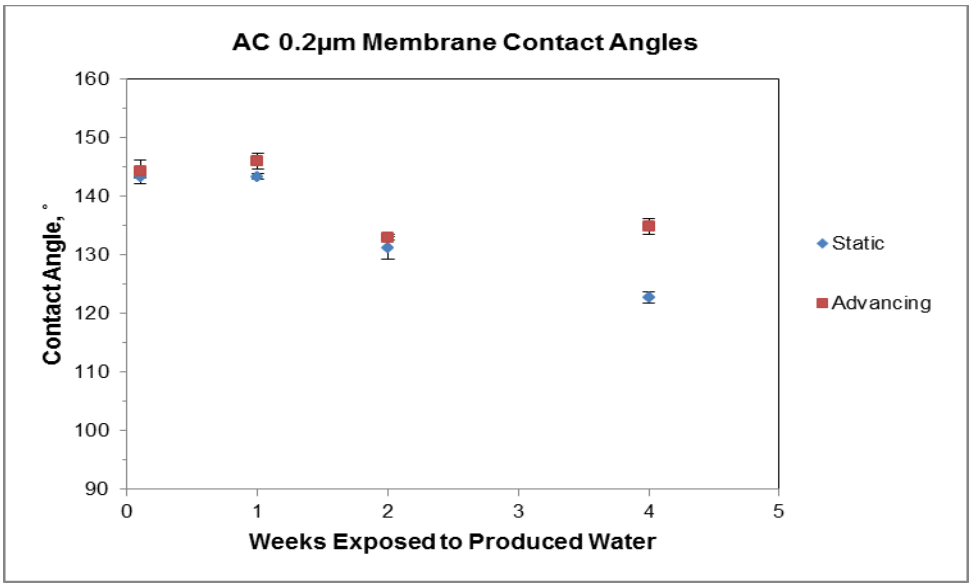

Figure 19. Contact Angle for 0.2 µm AC membrane after long-term exposure to produced water

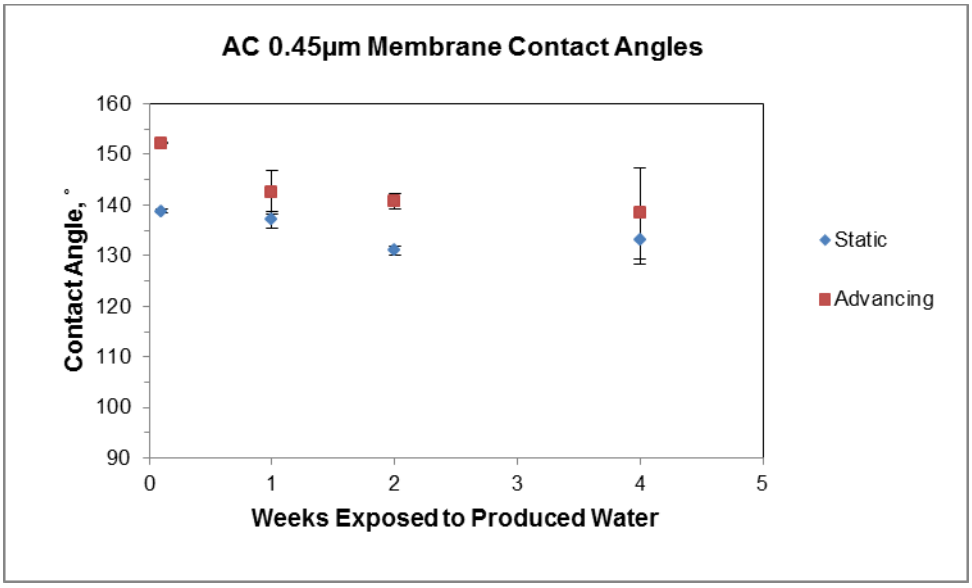

Figure 20. Contact Angle for 0.45 µm AC membrane after long-term exposure to produced water

Both the 0.2 and 0.45 µm pore size membranes remained hydrophobic after being in contact with heated A2 produced water in a closed environment. Results indicate that 0.2 µm pore size membrane appears to maintain initial hydrophobicity better than 0.45 µm membrane. The initial contact angle for the 0.2 µm pore size membrane exhibited at worst a 14% change

after 4 weeks of contact with produced water. Higher variability in contact angle observed from the 0.45 µm membrane could also be due to larger variability in membrane surface contour when compared to 0.2 µm membrane.

Despite a decrease in measured contact angle after 4 weeks of exposure to produced water, the membranes were still very hydrophobic. These results indicate that long term exposure to this particular produced water sample did not have significant detrimental effect on the integrity and hydrophobicity of acrylic copolymer.

4.3.2.2 LEP_w

Measuring the LEP_w of the exposed membrane samples, would both be a measure of membrane hydrophobicity and an indication of the structural durability of the membrane in a continuous DCMD operation. Unfortunately, the limited membrane samples from the floating tests prevented a complete and reliable of LEP_w. Issues with generating consistent LEP_w measurements likely stemmed from capillary forces prohibiting complete degassing of the measuring cell (filter holder) in the LEP apparatus on the onset of the process. During the LEP tests, it would appear that the LEP had been reached but an air bubble would be observed in the capillary tube and continuous flux could not be observed even at pressures above 450 kPa. A larger measuring cell and membrane sample was used for measuring the LEP_w when characterizing unused membranes. During those experiments, the measuring cell appeared to be effectively degassed. Thus the likelihood of obtaining reliable LEP measurements in a future iteration of the longevity experiment would require larger membrane samples.

5.0 SUMMARY AND CONCLUSIONS

The primary objectives of this study were to investigate the feasibility of MD as a final treatment method for flowback/produced waters and evaluate whether acrylic copolymer hydrophobic membranes are suitable for MD of flowback/produced water in terms of chemical compatibility and performance characteristics. The permeate flux measured in this study showed that the use of acrylic copolymer membranes for flowback and produced water treatment with DCMD is promising in terms of permeate flux that is comparable to the literature and RO flux rates. It is also promising for this application in terms of membrane fouling as well as compatibility with produced water chemistry. Overall the effects of temperature, feed salinity, and membrane pore size on permeate flux followed the governing theories for membrane distillation. Specific conclusions obtained in this study can be summarized as follows:

1. Permeate flux for AC membranes obtained with pure sodium chloride feed solution is comparable to that reported for other commercial hydrophobic membranes in DCMD applications. This confirms that AC membranes and the experimental module used in this study are suitable for DCMD testing.
2. There is a slight decrease in permeate flux with synthetic and real flowback and produced waters when compared to pure sodium chloride feed. This effect can be attributed to the divalent cations present in the synthetic and real flowback and produced water samples,

which can increase the number of solute moles by 19% compared to pure sodium chloride at the same TDS concentration. This increase in solute moles will decrease of the solution feed vapor pressure, which is the main driving force in MD.

3. The permeate flux decreased as the TDS increased for pure sodium chloride, synthetic flowback waters, and real flowback and produced waters. It appears that this trend is asymptotic as the decrease in permeate flux is dramatic at first and then it relatively stabilizes when TDS of the feed exceeds 15%, at which point the permeate flux decrease became more gradual with the salinity increase.
4. The DCMD performance did not vary greatly, especially at higher TDS of the feed, between 0.2 and 0.45 µm pore size AC membranes. This study showed that the 0.45 µm membrane has a higher affinity towards scaling than the 0.2 µm membrane, which is likely due to increased surface roughness and higher variability in the membrane surface elevation.
5. Membrane rinsing with DI water was able to restore clean water permeability following experimental runs of 100 minutes. Water contact angle measurements of membrane samples demonstrated that 4 weeks of continuous exposure to produced water did not have a significant adverse impact on the hydrophobicity of acrylic copolymer.

In conclusion, these results indicate that MD could be a technical solution that is an efficient treatment to manage Marcellus Shale flowback and produced waters for the oil and gas industry. Further research is warranted to confirm these results and to effectively scale the technology for full-scale implementation in the Marcellus Shale region and others.

6.0 FUTURE WORK

After analyzing the results of this research, there are three primary areas that would be worthwhile to pursue regarding the use of MD treatment of Marcellus Shale flowback and produced waters:

1. Further MD testing should be conducted with different actual flowback and produced water samples to confirm these initial results. This initial study was very limited and used sample water which was old (in some instances the samples used were collected two years prior to testing). A focus on produced waters should be more beneficial since there will be more produced water as the Marcellus Shale play is maturing and flowback water reuse has become industry disposal standard. Also, the TDS of produced water should be higher, which will further push the limits of the MD technology.
2. Further explore the most suitable membrane pore size for long-term use and answer the following questions: Will the 0.2 μm pore size continue to perform better with scaling and rinsing and will the difference in flux performance remain almost negligible? Are these initial trends attributable to the relative surface roughness between the 0.2 and 0.45 μm membranes?
3. Build a new DCMD module and experimental setup that will allow longer experimental runs.

The following gaps in the data generated during this study can be identified and the following issues should be considered in future MD tests with flowback and produced waters:

1. Total organic carbons (TOC) should be measured in the permeate side to observe and quantify whether there is any TOC passing through the membrane with the water vapors.
2. When assessing the relative hydrophobicity by measuring the contact angle with water also assess the relative oleophobicity by measuring the contact angle with hexadecane.
3. More regularly assess the clean water permeability measurements before and after tests to confirm rinsing protocol effectiveness and / or identify signs of membrane performance degradation.
4. Complete SEM/XRD analysis of membrane samples that were used with actual flowback and produced to identify changes in morphology and nature of deposits on the membrane surface.

APPENDIX A

CALCULATING MOLE FRACTION OF SOLVENTS

Raoult's law states that the vapor pressure of a solution is equal to the mole fraction (X_A) of the solvent multiplied by the vapor pressure of the pure solvent. Below the mole fraction of solvents is calculated for pure sodium chloride solution and synthetic A1 flowback solution. Both solutions have a TDS concentration of 3.9%.

1. **Calculating the mole fraction (X_A) for 1 L of 3.9% sodium chloride solution.**

   a. Calculating moles of solvent (H_2O)

$$\frac{1\ L\ H_2O \mid 988.039\ kg\ H_2O \mid 1\ m^3\ H_2O \mid 1{,}000\ g\ H_2O \mid 1\ mol\ H_2O}{\mid 1\ m^3\ H_2O \mid 1{,}000\ L\ H_2O \mid 1\ kg\ H_2O \mid 18\ g\ H_2O} = 54.89\ moles\ H_2O$$

   b. Calculating moles of solute particles (NaCl)

$$\frac{30.9\ g\ NaCl \mid 1\ mol\ NaCl \mid 2\ mol\ particles}{\mid 58.5\ g\ NaCl \mid 1\ mol\ NaCl} = 1.06\ moles\ particles$$

   c. Calculating the mole fraction (X_A)

$$X_{A,NaCl} = \frac{54.89\ moles\ H_2O}{54.89\ moles\ H_2O + 1.06\ mole\ particles} = \mathbf{0.981}$$

2. Calculating the mole fraction (X_A) for 1 L of 3.9% synthetic A1 solution

a. Calculating moles of solvent (H_2O) (initial)

54.89 moles H2O (from above)

b. Calculating moles of solute particles

i. NaCl

$$30.15\ g\ NaCl \left| \frac{1\ mol\ NaCl}{58.5\ g\ NaCl} \right| \frac{2\ mol\ particles}{1\ mol\ NaCl} = 1.03\ moles\ particles$$

ii. $CaCl_2$

$$8.12\ g\ CaCl_2 \cdot 2\ H_2O \left| \frac{111.1\ g\ CaCl_2}{147.1\ g\ CaCl_2 \cdot 2\ H_2O} \right| \frac{1\ mol\ CaCl_2}{111.1\ g\ CaCl_2} \left| \frac{3\ mol\ particles}{1\ mol\ CaCl_2} \right. = 0.17\ mole\ particles$$

iii. $MgCl_2$

$$1.84\ g\ MgCl_2 \cdot 6\ H_2O \left| \frac{95.3\ g\ MgCl_2}{203.3\ g\ MgCl_2 \cdot 6\ H_2O} \right| \frac{1\ mol\ MgCl_2}{95.3\ g\ MgCl_2} \left| \frac{3\ mol\ particles}{1\ mol\ MgCl_2} \right. = 0.027\ mole\ particles$$

iv. $BaCl_2$

$$1.39\ g\ BaCl_2 \cdot 2\ H_2O \left| \frac{208.3\ g\ BaCl_2}{244.3\ g\ BaCl_2 \cdot 2\ H_2O} \right| \frac{1\ mol\ BaCl_2}{208.3\ g\ BaCl_2} \left| \frac{3\ mol\ particles}{1\ mol\ BaCl_2} \right. = 0.017\ mole\ particles$$

v. $SrCl_2$

$$1.12\ g\ SrCl_2 \cdot 6\ H_2O \left| \frac{158.6\ g\ SrCl_2}{266.6\ g\ SrCl_2 \cdot 6\ H_2O} \right| \frac{1\ mol\ SrCl_2}{158.6\ g\ SrCl_2} \left| \frac{3\ mol\ particles}{1\ mol\ SrCl_2} \right. = 0.013\ mole\ particles$$

vi. Total moles of solute particles

Total solute mole particles = 1.03 + 0.17 + 0.027 + 0.017 + 0.013 = 1.26 mole particles

c. Calculating additional moles of solvent (H_2O) (from using hydrated salts)

$$\frac{8.12\ g\ CaCl_2 \cdot 2\ H_2O \mid 36\ g\ H_2O \mid 1\ mol\ H_2O}{\mid 147.1\ g\ CaCl_2 \cdot 2\ H_2O \mid 18\ g\ H_2O} = 0.11\ mole\ H_2O$$

$$\frac{1.84\ g\ MgCl_2 \cdot 6\ H_2O \mid 108\ g\ H_2O \mid 1\ mol\ H_2O}{\mid 203.3\ g\ MgCl_2 \cdot 6\ H_2O \mid 18\ g\ H_2O} = 0.054\ mole\ H_2O$$

$$\frac{1.39\ g\ BaCl_2 \cdot 2\ H_2O \mid 36\ g\ H_2O \mid 1\ mol\ H_2O}{\mid 244.3\ g\ BaCl_2 \cdot 2\ H_2O \mid 18\ g\ H_2O} = 0.011\ mole\ H_2O$$

$$\frac{1.12\ g\ SrCl_2 \cdot 6\ H_2O \mid 108\ g\ H_2O \mid 1\ mol\ H_2O}{\mid 266.6\ g\ SrCl_2 \cdot 6\ H_2O \mid 18\ g\ H_2O} = 0.025\ mole\ H_2O$$

$$Total\ solvent\ mole\ particles\ from\ hydrated\ salts = 0.11 + 0.054 + 0.011 + 0.025 = 0.20\ mole\ H_2O$$

$$Total\ solvent\ mole\ particles = 54.89 + 0.20 = 55.09\ mole\ H_2O$$

d. Calculating the mole fraction (X_A)

$$X_{A,SynA1} = \frac{55.09\ moles\ H_2O}{55.09\ moles\ H_2O + 1.26\ mole\ particles} = \mathbf{0.978}$$

In conclusion, according to Raoult's Law since $X_{A,NaCl} > X_{A,SynA1}$ the vapor pressures of the 3.9% NaCl solution will be marginally higher than the vapor pressure of the 3.9% synthetic A1 solution at the same temperature.

BIBLIOGRAPHY

Adnan, S., Hoang, M., Wang, H., Xie, Z., (2012). Commercial PTFE membranes for membrane distillation application: Effect of microstructure and support material. *Desalination,* Vol. 284, pp. 297-308.

Alkhudhiri A., Darwish, N., Hilal, N., (2012). Membrane distillation: A review. *Desalination,* Vol. 287, pp. 2-18.

Alklaibi, A.M., Lior, N., (2005). Membrane-distillation desalination: status and potential. *Desalination,* Vol. 171, pp. 111-131.

Al-Obaidani, S., Curcio, E., Macedonio, F., Drioli, E., (2008). Potential of membrane distillation in sweater desalination: Thermal efficiency, sensitivitiy study and cost estimation. *Journal of Membrane Science,* Vol. 323, pp. 85-98.

Bonyadi, S., Chung, T.S., (2007). Flux enhancement in membrane distillation by fabrication of dual layer hydrophilic-hydrophobic hollow fiber membranes. *Journal of Membrane Science,* Vol. 306, pp. 134-146.

Cath, T.Y., Adams, V.D., Childress, A.E., (2004). Experimental study of desalination using direct contact membrane distillation: a new approach to flux enhancement. *Journal of Membrane Science,* Vol. 228, pp. 5-16.

Colorado School of Mines, (2009). Technical assessment of produced water treatment technologies. *RPSEA Project 07122-12.*

Dores, R., Hussain, A., Katebah, M., Adham, S., (2012). Using advanced water treatment technologies to treat produced water from the petroleum industry. *Society of Petroleum Engineers,* SPE International Production and Operations Conference and Exhibition.

Franken, A.C.M., Nolten, J.A.M., Mulder, M.H.V., Bargeman, D., Smolders, C.A., (1987). Wetting criteria for the applicability of membrane distillation. *Journal of Membrane Science,* Vol. 33, pp. 315-328.

Gryta, M., (2008). Fouling in direct contact membrane distillation process. *Journal of Membrane Science,* Vol. 325, pp. 383-394.

Hanemaaijer, J.H., van Medevoort, J., Jansen, A.E., Dotremont, C., van Sonsbeek, E., Yuan, T., De Ryck, L., (2006). Memstill membrane distillation – a future desalination technology. *Desalination*. Vol. 199, pp. 175-176.

Hayes, T.D., (2009). Sampling and analysis of water streams associated with the development of Marcellus shale gas. *Gas Technology Institute, Des Plaines IL,* Final Report to the Marcellus Shale Coalition.

He, C., Wang, X., Liu, W., Barbot, E., Vidic, R.D., (2014). Microfiltration in recycling of Marcellus Shale flowback water: Solids removal and potential fouling of polymeric microfiltration membranes. *Journal of Membrane Science,* Vol. 462, pp. 88-95.

Holman, J.P., (1986). *Heat Transfer.* Sixth Edition, McGraw-Hill.

Izquierdo-Gil, M.A., Fernández-Pineda, C., Lorenz, M.G., (2008). Flow rate influence on direct contact membrane distillation experiments: Different empirical correlations for Nusselt number. *Journal of Membrane Science,* Vol. 321, pp. 356-363.

Ji, X., Curcio, E., Al Obaidani, S., Di Profio, G., Fontananova, E., Drioli, E., (2010). Membrane distillation-crystallization of seawater reverse osmosis brines. *Separation and Purification Technology*, Vol. 71, pp. 76-82.

Kays, W. M., Crawford, M.E., (1993). *Convective Heat and Mass Transfer.* Third Edition, McGraw-Hill.

Khayet, M., (2011). Membranes and theoretical modeling of membrane distillation: A review. *Advances in Colloid and Interface Science,* Vol. 164, pp. 56-88.

Khayet, M., Velázquez, A., Mengual, J.I., (2004). Direct contact membrane distillation of humic acid solutions. *Journal of Membrane Science,* Vol. 240, pp. 123-128.

Laganà F., Barbieri, G., Drioli, E., (2000). Direct contact membrane distillation: modelling and concentration experiments. *Journal of Membrane Science,* Vol. 166, pp. 1-11.

Lawson, K.W., Lloyd, D.R., (1996). Membrane distillation. II. Direct contact MD. *Journal of Membrane Science,* Vol. 120, pp. 123-133.

Lawson, K.W., Lloyd, D.R., (1997). Review: membrane distillation. *Journal of Membrane Science,* Vol. 124, pp. 1-25.

Macedonio, F., Curcio, E., Drioli, E., (2007). Intergrated membrane systems for seawater desalination: energetic and exergetic analysis, economic evaluation, experimental study. *Desalination,* Vol. 203, pp. 260-276.

Macedonio, F., Drioli, E,, (2010). An exergetic analysis of a membrane desalination system1. *Desalination,* Vol. 261, pp. 293-299.

Martinetti, C.R., Childress, A.E., Cath, T.Y., (2009). High Recovery of concentrated RO brines using forward osmosis and membrane distillation. *Journal of Membrane Science,* Vol. 331, pp. 31-39.

Martínez-Díez, L., Florido-Díaz, F.J., (2001). Desalination of brines by membrane desalination. *Desalination,* Vol. 137, pp. 267-273.

Nghiem, L.D., Cath, T., (2011). A scaling mitigation approach during direct contact membrane distillation. *Separation and Purification Technology,* Vol. 80 (2), pp. 315-322.

Ohio Department of Natural Resources Division of Oil & Gas Resources, (updated October 3, 2016).http://oilandgas.ohiodnr.gov/portals/oilgas/pdf/Class%20II%20Brine%20Injection%20Wells%20of%20Ohio%2010032016.pdf, (retrieved October 14, 2016).

Ohio Quakes Probably Triggered by Waste Disposal Well, Say Seismologists, (January 6, 2012). https://www.ldeo.columbia.edu/news-events/seismologists-link-ohio-earthquakes-waste-disposal-wells, (retrieved October 14, 2016).

Panin, G.N., Brezgunov, V.S., (2007). Influence of the salinity of water on its evaporation. *Izvestiya, Atmospheric and Oceanic Physics,* Vol. 43, pp. 718-720.

Pennsylvania Department of Environmental Protection. http://www.dep.pa.gov/DataandTools/Reports/Oil%20and%20Gas%20Reports/Pages/default.aspx, (retrieved October 14, 2016).

P.J. Linstrom and W.G. Mallard, Eds., (2016). NIST Chemistry WebBook, NIST Standard Reference Database Number 69, *National Institute of Standards and Technology, Gaithersburg MD,* http://webbook.nist.gov, (retrieved January 24, 2016).

Clynne, M.A., Potter, R.W., (1979). Solubility of some alkai and alkaline earth chlorides in water at moderate temperatures. *Journal of Chemical & Engineering Data*. Vol. 24, pp. 338-340.

Schofield, R.W., Fane A.G., Fell C.J.D., (1987). Heat and mass transfer in membrane distillation. *Journal of Membrane Science,* Vol. 33, pp. 299-313.

Schoefield R.W., Fane A.G., Fell C.J.D., Macoun R., (1990). Factors affecting flux in membrane distillation. *Desalination,* Vol. 77, pp. 279-294.

Silva, J.M., Gettings, R.M., Kostedt, W.L., Watkins, V.H., Hardy, A., Shapiro, A., (2014). NORM Mitigation and Clean Water Recovery from Marcellus Produced Water. *RPSEA Contract 10122-07*.

Singh, D., Sirkar, K.K., (2012). Desalination of brine and produced water by direct contact membrane distillation at high temperatures and pressures. *Journal of Membrane Science,* Vol. 389, pp. 380-388.

Sirkar K.K., Li, B., (2003). Novel membrane and device for direct contact membrane distillation-based desalination process: Phase II. US Department of the Interior, Bureau of Reclamation.

Sirkar, K.K., Song, L., (2009). Pilot-scale studies for direct contact membrane distillation-based desalination process. US Department of the Interior, Bureau of Reclamation.

Sharqawy, M.H., Leinhard, J.H., Zubair, S.M., (2010). Thermophysical properties of seawater: a review of existing correlations and data. *Desalination and Water Treatment,* Vol. 16, pp. 354-380.

Smolders, K., Franken, A.C.M., (1989). Terminology for Membrane Distillation. *Desalination,* Vol. 72, pp. 249-262.

Song, L., Ma, Z., Liao, X., Kosaraju, P.B., Irish, J.R., Sirkar, K., (2008). Pilot plant studies of novel membranes and devices for direct contact membrane distillation-based desalination. *Journal of Membrane Science,* Vol. 323, pp. 257-270.

Tun, C.M., Fane, A.G., Matheickal, J.T., Sheikholeslami, R., (2005). Membrane distillation crystallization of concentrated salts – flux and crystal formation. *Journal of Membrane Science,* Vol. 257, pp. 144-155.

Walton, J., Lu, H., Turner, C., Solis, S., Hein, H., (2004). Solar and waste heat desalination by membrane distillation. *Desalination and Water Purification Research and Development Program Report No. 81*. U.S. Department of the Interior Bureau of Reclamation. Agreement No. 98-FC-81-0048.

Wang, P., Teoh, M.M., Chung, T., (2011). Morphological architecture of dual-layer hollow fiber for membrane distillation with higher desalination performance. *Water Research,* Vol. 45, pp. 5489-5500.

Wang, K.Y., Chung, T., Gryta, M., (2008). Hydrophobic PVDF hollow fiber membranes with narrow pore size distribution and ultra-thin skin for the fresh water production through membrane distillation. *Chemical Engineering Science,* Vol. 63, pp. 2587-2594.

Wirth, D., Cabassud, C., (2002). Water desalination using membrane distillation: comparison between inside/out and outside in permeation. *Desalination,* Vol. 147, pp. 139-145.

Yun, Y., Ma, R., Zhang, W., Fane, A.G., Li, J., (2006). Direct contact membrane distillation mechanism for high concentration NaCl solutions. *Desalination,* Vol. 188, pp. 251-262.

(n.d.). Retrieved from February 7, 2016, from http://www.solarspring.de/index.php?id=19

(n.d.). Retrieved from February 7, 2016, from http://bluegoldtech.com/technology/, 2016

(n.d.). Retrieved from February 7, 2016, from http://www.keppelseghers.com/en/content.aspx?sid=3023

(n.d.). Retrieved from February 7, 2016, from http://www.memsys.eu/

(n.d.). Retrieved from February 7, 2016, from http://www.aquaver.com/

(n.d.). Retrieved from February 7, 2016, from http://www.memsys.eu/partners-details/ge.html

(n.d.). Retrieved from February 7, 2016, from http://www.chemicalprocessing.com/vendor-news/2013/ge-and-memsys-field-project-shows-promise-for-treatment-of-fracking-wastewater/

(n.d.). Retrived from February 7, 2016, from http://www.hvr.se/Products.html